Drug Carriers

International Edition: DOI: 10.1002/anie.201503054
German Edition: DOI: 10.1002/ange.201503054

Stimuli-Responsive DNA-Functionalized Nano-/Microcontainers for Switchable and Controlled Release

*Chun-Hua Lu and Itamar Willner**

Keywords:
lipid–DNA micelles · mesoporous nanoparticles · microcapsules · nanomedicine · vesicles

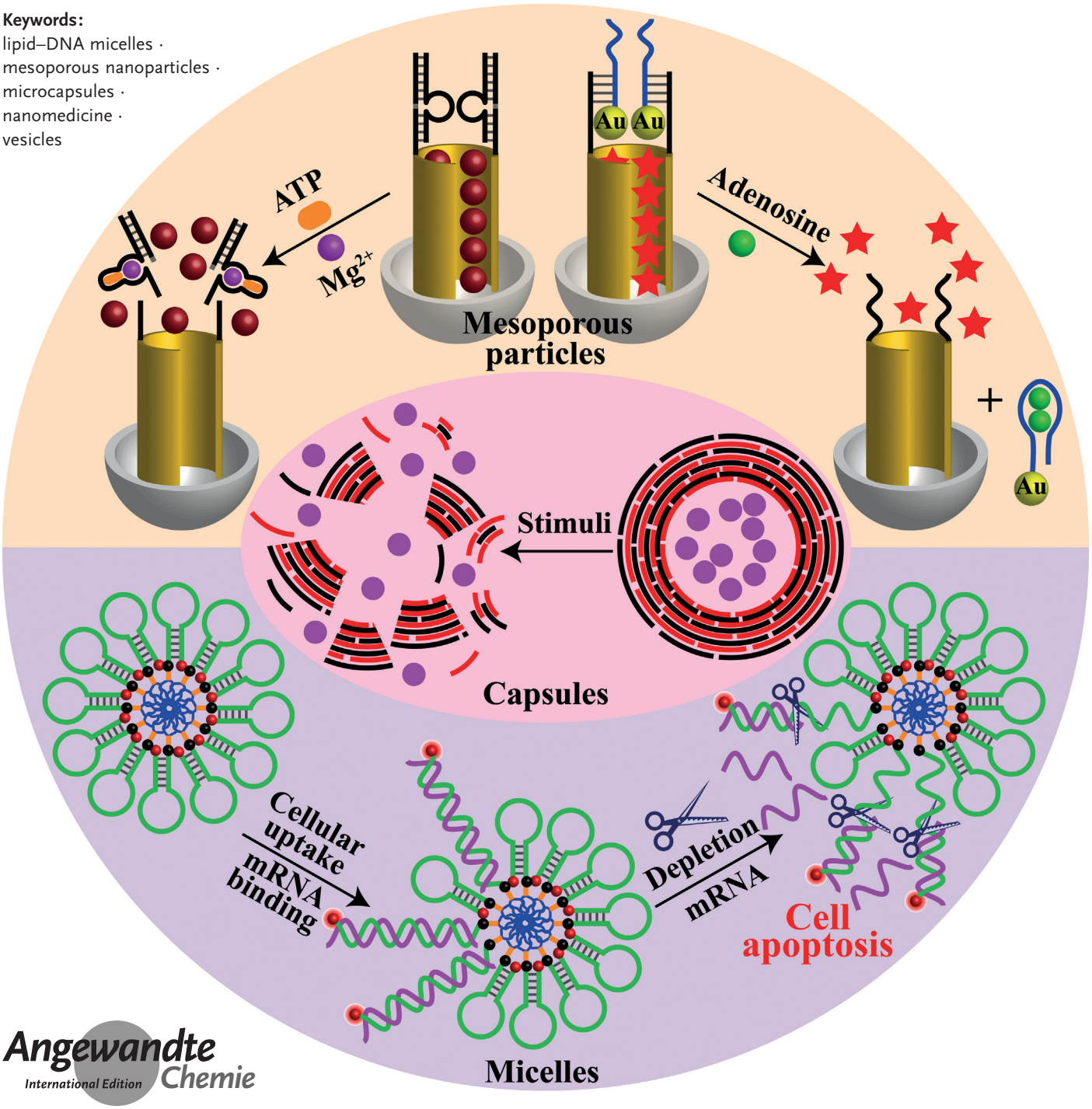

Stimuli-responsive DNA-functionalized nano- and microcontainers composed of mesoporous SiO_2 nanoparticles (MP SiO_2 NPs), microcapsules, or micelles/vesicles act as carriers for the transport and release of drugs. The information encoded in the DNA sequences provides instructive information for the gating of drug-loaded pores of MP SiO_2 NPs, for the assembly and degradation of microcapsules or lipid–DNA micelles/vesicles, and for the targeting of nano-/microcontainers to cancer cells. Different triggers are applied to release the drugs loaded in the nano-/microcontainers by unlocking the pores of the MP SiO_2 NPs or by degradation of the containers. These include the use of switchable DNA nanostructures (nucleic acid hairpins, i-motif, G-quadruplexes) and the implementation of chemical, thermal, or photonic stimuli. Also, catalytic processes stimulated by DNAzymes or enzymes are used to release drugs from the nano-/microcontainers.

From the Contents

1. Introduction

The base sequence of oligonucleotides (DNA) encodes substantial structural and functional information in the biopolymer. Besides the well-established base-pairing of A-T and G-C bases to form duplex nucleic acids, the base-dictated self-assembly of nucleic acids into different nanostructures is of interest[1] (Figure 1 A). DNA strands that include self-complementarity generate hairpin structures, cytosine (C)-rich strands assemble under appropriate pH-conditions into i-motif structures,[2] and guanosine (G)-rich sequences self-assemble in the presence of K^+ or NH_4^+ ions into G-quadruplex nanostructures.[3] Also, appropriate base-domains, such as T-A·T or C-G·C, allow the formation of triplex DNA structures.[4] Similarly, metal ions bridge nucleotide bases to form T-Hg^{2+}-T or C-Ag^+-C complexes, and different intercalators bind to duplex DNA strands.[5,6] These complexes cooperatively stabilize DNA duplexes or other nucleic acid nanostructures. The different oligonucleotide nanostructures can be separated under appropriate conditions; duplex DNA undergoes strand displacement to form energetically stabilized structures,[7] hairpin nucleic acids open upon hybridization of nucleic acids with the loop region of the hairpins,[8] i-motif structures dissociate at neutral pH to random coils, triplex DNA assemblies are separated at different pH values, and G-quadruplexes or metal-ion-bridged duplexes are separated by ligand-induced elimination of the ions stabilizing the structures.[9,10] Similarly, photoisomerizable units exhibit switchable binding properties to duplex DNA, resulting in switchable cooperative stabilization of double-stranded DNA nanostructures. For example, *trans*-azobenzene units intercalate into double-stranded DNA, resulting in the stabilization of the duplex structures. Photoisomerization of the *trans*-azobenzene units into *cis*-azobenzene units that lack intercalation affinities toward duplex DNA results in the weakening, and eventually, the separation of the double-stranded structures.[11] Oligonucleotides may also reveal specific recognition properties. Sequence-specific nucleic acids with high-affinity binding properties to low-molecular-weight substrates, macromolecules (e.g., proteins), and even to cells are available (aptamers)[12] and can be elicited by the systematic evolution of ligands by exponential enrichment (SELEX) process.[13] Also, many sequence-specific nucleic acids exhibit catalytic properties (DNAzymes), such as metal-ion-dependent DNAzymes[14] or the hemin/G-quadruplex horseradish-peroxidase mimicking DNAzyme.[15] Different enzymes react with DNA (Figure 1 B). Polymerase replicates in the presence of the dNTPs mixture, a primer nucleic acid hybridized with a DNA scaffold,[16] sequence-specific endonucleases cleave duplex DNA structures,[17] sequence-specific nicking enzymes cleave a single-strand target site in duplex DNA structures,[18] DNase digests DNA strands, and exonucleases, such as exonuclease III (Exo III), hydrolytically digest the 3′-end of a duplex DNA strand.[19]

The possibilities to trigger structural transitions of DNA nanostructures by means of environmental stimuli or catalytic transformations provide a rich arsenal of tools to manipulate DNA. The reconfiguration of DNA nanostructures by environmental stimuli,[20] the recognition properties of aptamers,[12] the catalytic functions of DNAzymes, and the biocatalytic reactions on nucleic acid structures[14,15] have a tremendous impact on the development of different topics in the rapidly developing area of DNA nanotechnology. The development of DNA switching systems,[20] DNA-based machines,[21] amplified DNA-sensing platforms,[22,23] and the application of DNA as a functional material for operating logic-gate and computing circuits[24,25] make use of these unique features of DNA. The present Review discusses the use of DNA hybrid systems as stimuli-responsive carriers for the controlled release of payloads. Specifically, stimuli-responsive DNA-functionalized mesoporous nanoparticles

[*] Dr. C. H. Lu, Prof. I. Willner
Institute of Chemistry, The Hebrew University of Jerusalem
Jerusalem 91904 (Israel)
E-mail: willnea@vms.huji.ac.il
Homepage: http://chem.ch.huji.ac.il/willner/

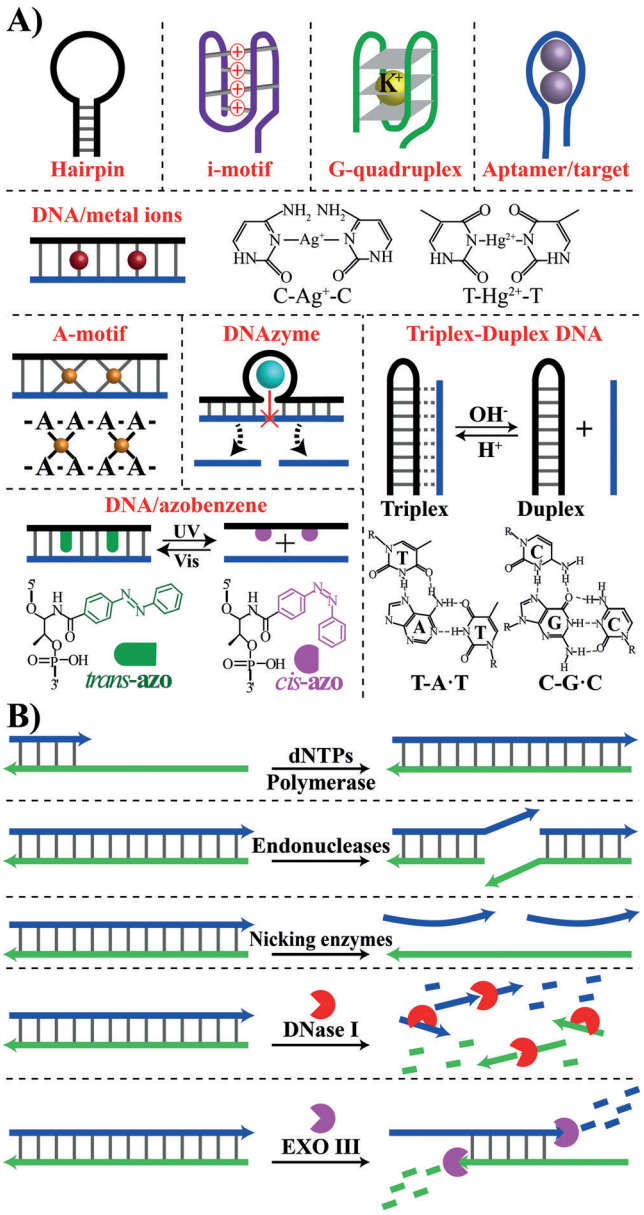

Figure 1. A) Self-assembly of DNA nanostructures and complexes by environmental stimuli or co-added ligands/ions. B) Examples of bio-catalyzed transformations occurring on DNA nanostructures.

(NPs), DNA-based micro-/nanocapsules, and micelles and vesicles consisting of lipid–nucleic acid conjugates are addressed. The methods to assemble the stimuli-responsive DNA-based containers, the mechanisms to trigger the unlocking of these micro-/nanoreservoirs and the release of payloads, and the future applications of these systems for sensing and for targeted and controlled drug release in nanomedicine are presented.

2. DNA-Capped Mesoporous Nanoparticles for Controlled Release

Mesoporous particles are defined as nanoparticles that include pores with diameter between 2 nm and 50 nm. Many different inorganic materials such as carbon, TiO_2, and SiO_2, were prepared in the form of mesoporous micro- or nanoparticles.[26,27] These rigid mesoporous particles exhibit important features, such as high surface area and loading capacity, biocompatibility, chemical stability, and surface functionalities that allow chemical modification of the surface as well as uptake of the particles into cells. Many different applications of substrate-loaded mesoporous particles were suggested, including sensing,[28] drug delivery,[29] imaging,[30] and catalysis.[31]

For the biomedical application of mesoporous NPs, specifically mesoporous SiO_2 nanoparticles (MP SiO_2 NPs), as drug delivery vehicles, the NPs have to fulfill several prerequisites: 1) The pores need to be loaded with the drug cargo (or a model analogue) and capped by functional units that prevent or minimize uncontrolled release. 2) The pore-capping units should be unlocked by external or environmental triggers, allowing the controlled release of the load. 3) Surface modifiers on the NPs should allow the targeting of the NPs to specific cells and facilitate cellular endocytosis. The unlocking of the pores by specific intracellular biomarkers or chemical agents is advantageous for targeted controlled release. Indeed, substantial research efforts have been directed to develop stimuli-responsive capped MP SiO_2 NPs. These include the unlocking of the caps by pH-triggers,[32] chemical stimuli[33] such as glucose, the implementation of redox-active caps[34,35] such as disulfide or quinone caps, the use of photonic signals,[36] the application of thermal[37] or

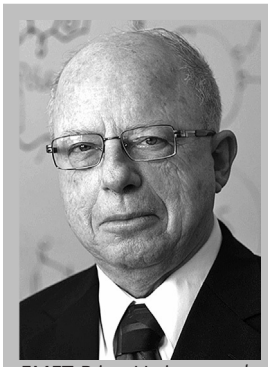

Itamar Willner completed his Ph.D. studies at The Hebrew University of Jerusalem in 1978. After postdoctoral research (1978–1981) at U.C. Berkeley, he joined the Institute of Chemistry at The Hebrew University of Jerusalem, where he was appointed as Professor in 1986. His research interests include bioelectronics and molecular electronics, nanobiotechnology, sensors and biosensors, artificial photosynthesis and the development of stimuli-responsive materials. He is the recipient of the Israel Prize in Chemistry, the Rothschild Prize, and the EMET Prize. He is a member of the Israel Academy of Sciences, the German National Academy of Sciences, Leopoldina, and the European Academy of Sciences and Arts.

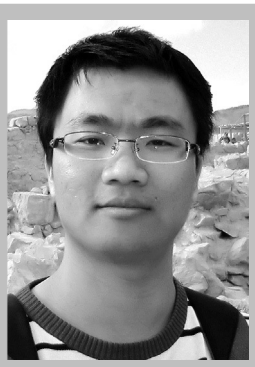

Dr. Chun-Hua Lu is currently a postdoctoral research associate in the laboratory of Prof. Itamar Willner, Institute of Chemistry, The Hebrew University of Jerusalem. He received his B.S. (2005) and Ph.D. (2011) degrees from College of Chemistry and Chemical Engineering, Fuzhou University, China. His research interests address topics of DNA nanotechnology, including DNA machines, plasmonic effects using DNA/metal nanoparticle structures, and DNA hydrogels.

magnetic fields,[38] and the use of enzymes as catalysts for the degradation of the caps.[39] The release of different drugs such as insulin[40] or chemotherapeutic drugs[41] was demonstrated. Several excellent Review articles have discussed recent advances in the application of stimuli-controlled mesoporous NPs for controlled drug delivery.[42]

Nucleic-acid-functionalized mesoporous NPs exhibit attractive features for triggered drug delivery: 1) Bulky DNA nanostructures generated by bridged duplexes, polymerized DNA chains (by the hybridization chain reaction, HCR, or polymerase-induced replication), the assembly of two- or three-dimensional DNA structures, or the formation of aptamer–ligand complexes provide effective nanostructures for capping the pores. 2) Different triggers including strand displacement,[7] pH,[9] ligands,[10] or thermal stimuli[43] could reconfigure the capping units resulting in the unlocking of the pores and the release of entrapped substrates. 3) Enzymatic or DNAzyme-catalyzed cleavage of DNA caps might provide means to unlock the caps and release the pore-entrapped loads. 4) Sequence-specific aptamers that specifically bind to cells (e.g., cancer cells), or receptor-biomarkers associated with cells, are known. The modification of mesoporous NPs with such aptamers may target the drug-loaded NPs to specific cells, and facilitate their cellular endocytosis and targeted release of the drug. The present section will address the use of DNA-modified mesoporous NPs as functional stimuli-responsive hybrids for controlled drug release.

Bulky stimuli-responsive DNA nanostructures have been widely implemented to cap substrates in the pores of mesoporous NPs and to release the pore-entrapped materials in the presence of appropriate unlocking triggers. For example, duplex DNA structures have been applied as pore-capping units, and their separation by different triggers was reported.[44] Figure 2 A outlines the unlocking of duplex-capped MP SiO_2 NPs, loaded with rhodamine B (RhB) as a model drug, using temperature or enzymatic digestion of the caps as unlocking triggers. Azide-functionalized MP SiO_2 NPs were loaded with RhB, and the pores were capped by reacting the NPs with the self-complementary duplex of the alkyne-modified nucleic acid **1**/**1** using click chemistry. The thermal dissociation of the duplex-DNA capping units or the enzymatic digestion of the units in the presence of DNase I unlocked the pores, thus triggering the release of the fluorescent load as shown in Figure 2 B and C, respectively. Similarly, the anticancer drugs camptothecin (CPT) and floxuridine (FUDR) were loaded into the MP SiO_2 NPs and capped with the duplex DNAs. In vitro experiments (human liver cancer cells; HepG2) showed that effective uptake of the CPT-loaded MP SiO_2 NPs by the cancer cells occurred. For this purpose, the fluorescent CPT drug ($\lambda = 423$ nm) was loaded in the pores, and the surface of the NPs was modified with fluorescein isothiocyanate as fluorescent label, $\lambda =$ 519 nm. The fluorescence of the drug and label enabled to follow the endocytosis and drug release events. It was found that the DNA-capped CPT-loaded MP SiO_2 NPs were effectively internalized in the cancer cells, and the endonucleases present in the cells triggered the unlocking and release of the drug, resulting in the effective killing of the cells

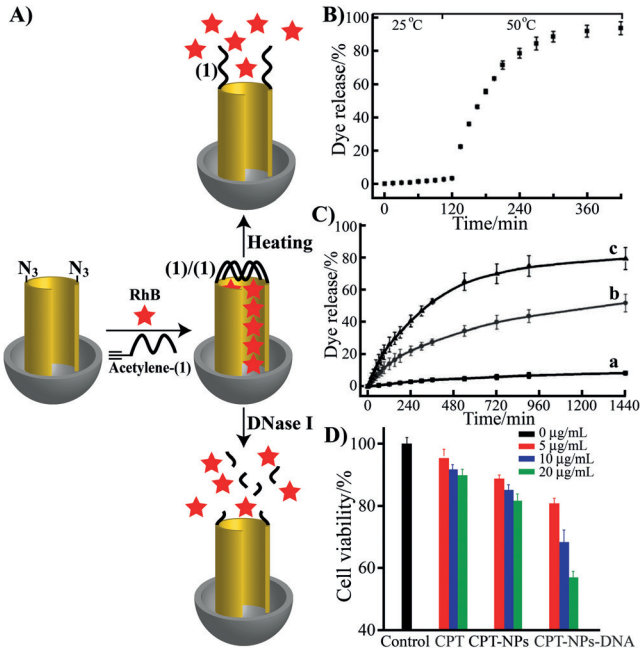

Figure 2. A) RhB-loaded duplex-DNA-capped MP SiO_2 NPs as stimuli-responsive load/release material. The unlocking of the pores occurs by thermal dissociation of the capping units or hydrolytic digestion of the caps by DNase I. B) Time-dependent thermally stimulated release of the RhB load. C) Time-dependent release of the RhB load in the presence of variable concentrations of DNase I: a) Without enzyme; b) 10 U ml^{-1}; c) 20 U ml^{-1}; D) HepG2 cancer-cell viability in the presence of CPT-loaded MP SiO_2 NPs, capped with the duplex DNA being unlocked by intracellular enzymes. The cells are treated with variable concentrations of the CPT drug, and compared to different control systems. Adapted with permission from Ref. [44]. Copyright 2011 Wiley-VCH.

(Figure 2 D). In a related study, other enzymes, such as Exo III or the nicking enzyme Nb.BbvCI, were used to unlock substrate-loaded MP SiO_2 NPs capped with duplex DNA units.[45] These systems represent potential sense-and-treat nanoparticle devices, because with the appropriate design of the hairpins, a defective disease-causing gene might trigger the release of a drug (e.g., an anticancer chemotherapeutic drug).

The unlocking of MP SiO_2 NPs by the reconfiguration of DNA caps through the formation of an aptamer–ligand complex and the subsequent biocatalytic exonuclease-stimulated digestion of the resulting aptamer complex, was implemented for the controlled release of the anticancer drug CPT into breast cancer cells[45] (Figure 3 A). The system made use of the fact that ATP is overproduced in cancer cells and that the exonuclease-type nicking enzyme EndoGI is present in cancer cells.[46] Accordingly, the MP SiO_2 NPs were functionalized with the DNA hairpin structure **6** that includes the anti-ATP aptamer sequence, domain I, in the hairpin structure. The thermal dissociation of the hairpin structure to a random coil enabled the loading of the pores with CPT. The locking of the anticancer drug CPT was achieved by cooling the system and capping the pores with the bulky hairpin units. In the presence of ATP, the hairpin-capping unit reconfigured into the ATP–aptamer complex structure that included an

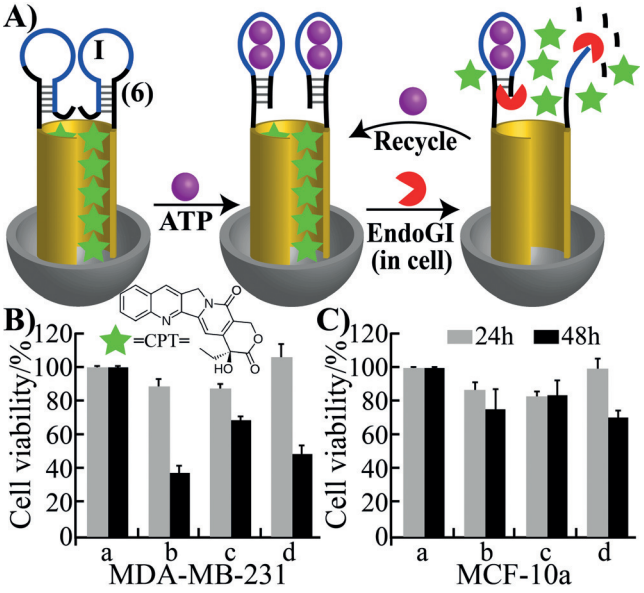

Figure 3. A) Probing the viability of MDA-MB-231 breast cancer cells, and of the MCF-10a normal breast cells, subjected to CPT-loaded MP SiO_2 NPs capped with hairpin DNA nanostructures. The hairpins contain the ATP aptamer sequence in the domain I. In the presence of ATP, which is overexpressed in cancer cells, and EndoGI, which is an exonuclease-type enzyme present in cancer cells, the hairpin caps reconfigure into the aptamer–ATP complex units that are digested by EndoGI, resulting in the release of CPT. B) Cell viability of the MDA-MB-231 breast cancer cells, and C) cell viability of MCF-10a normal breast cells after of 24 h (gray) and 48 h (black), corresponding to: a) Untreated cells; b) CPT-loaded MP SiO_2 NPs; c) free CPT-treated cells; d) oligomycin-treated cells (for inhibition of ATP production), in the presence of CPT-loaded MP SiO_2 NPs. Adapted with permission from Ref. [45]. Copyright 2013 American Chemical Society.

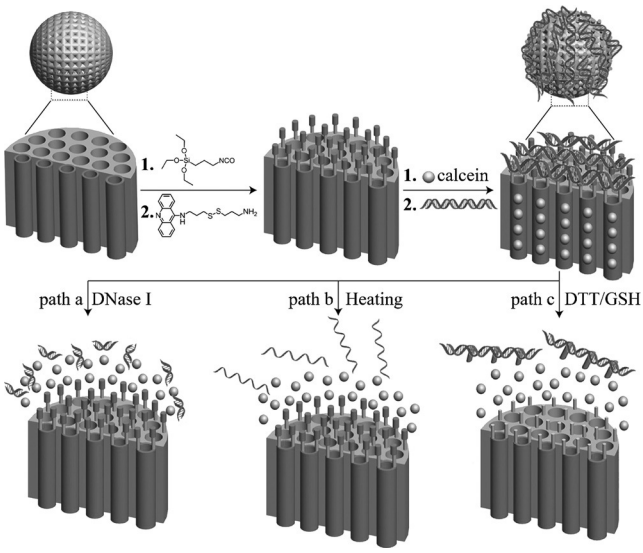

Figure 4. Synthesis of calcein-loaded MP SiO_2 NPs capped with surface-modified 9-acridinamine disulfide units intercalating into the duplex DNA structure. Unlocking of the pores and release of the loads is stimulated by the separation of the intercalator–duplex DNA caps: Path (a) by DNase I digestion of the duplex DNAs; path (b) by thermal separation of the duplex DNAs; path (c) by thiol-mediated cleavage of the disulfide bonds linking the intercalator units to the NPs. Adapted with permission from Ref. [48]. Copyright 2013 Wiley-VCH.

active 3′-ended duplex domain recognized by the EndoGI enzyme. The cleavage of the duplex domain separated the ATP–ligand complex, regenerated the ATP biomarker for further reconfiguring of the hairpin units, and resulted in the release of the anticancer drug CPT. The CPT-loaded MP SiO_2 NPs were introduced into MDA-MB-231 breast cancer cells, and into MCF-10a normal breast cells. The effects of the CPT-loaded NPs on the two types of cells are displayed in Figure 3B and C, respectively. Whereas the viability of the breast cancer cells decreased by 65% upon treatment of the cells with the drug-loaded MP SiO_2 NPs for a time interval of 48 h, the viability of the normal cells decreased only by 20% upon treatment with the drug-loaded MP SiO_2 NPs under similar conditions. These results are consistent with the overproduction of ATP in cancer cells, which leads to an enhanced release of the drug in cancerous cells. The function of ATP in unlocking the pores was further supported by treatment of the cells that contained the CPT-loaded MP SiO_2 NPs with oligomycin, a suppressor of ATP generation in cells.[47] Under these conditions the cell viability decreased to only 50%, consistent with the lower ATP-driven release of the drug. Also, it was found that the CPT-loaded MP SiO_2 NPs revealed a superior effect on cancer cell death, as compared to cells treated with free CPT, presumably due to effective endocytosis of the MP SiO_2 NPs into the cancer cells.

A different approach to gate and unlock MP SiO_2 NPs by means of duplex DNA structures has applied a molecularly engineered 9-acridinamine intercalator as functional unit to cap the pores and trigger their unlocking[48] (Figure 4). The 9-acridinamine derivative was covalently attached to MP SiO_2 NPs. It includes the acridine amine intercalator site that binds to duplex DNA, and a cleavable disulfide bond. The 9-acridinamine disulfide-modified MP SiO_2 NPs were loaded with calcein and the pores were capped by duplex DNA units through supramolecular binding of the intercalator units to the duplex DNA. The unlocking of the pores and release of the entrapped calcein was then stimulated by three different triggers. By one mechanism, treatment of the system with DNase I resulted in the digestive cleavage of the duplex, resulting in the separation of the caps, and the release of the calcein load [path (a)]. A different mechanism [path (b)] has applied the thermal dissociation of the duplex-capping units and the release of the load. A third, chemically stimulated unlocking of the pores has involved the reaction of the intercalator/duplex DNA-capped MP SiO_2 NPs with dithiothreitol (DTT) or the biologically active glutathione (GSH). The thiols trigger the reductive cleavage of the disulfide bridges leading to the separation of the intercalator/DNA duplex caps, and the release of calcein [path (c)]. Other methods to cap MP SiO_2 NPs by nucleic acids have involved the electrostatic adsorption of single-stranded DNA on positively-charged amine-functionalized NPs, and the removal of the blocking DNA locks by the formation of energetically stabilized duplexes.[49]

DNA-capped MP SiO_2 Fe_3O_4@Au NPs were loaded with the anticancer drug doxorubicin (DOX) and used as stimuli-responsive nanomaterial affecting the viability and growth of

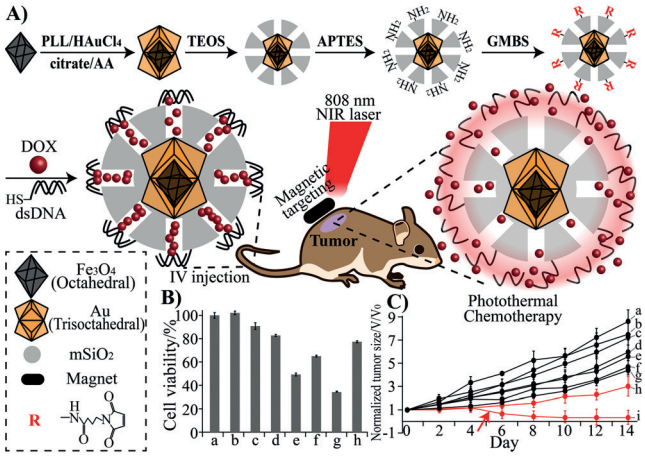

Figure 5. A) Synthesis and application of Fe_3O_4@Au core–shell nanoparticles coated with a mesoporous SiO_2 layer, loaded with DOX, and capped with a thiol-modified duplex DNA, for the magnetic targeting and thermal treatment of the cancer cells or HeLa tumors in mice. The Fe_3O_4 magnetic NPs provide a means to direct and localize the drug carrying NPs by an external magnetic field. The Au coating of the NPs provides a plasmonic layer for the thermal dissociation of the duplex-DNA capping units, and for the release of the drug. B) Viability of HeLa cells after 24 h, and examined upon: a) Cells with no additive; b) the cells treated only with laser irradiation (10 min exposed to laser irradiation $\lambda = 808$ nm, power 3 $W cm^{-2}$); c) in the presence of the DOX-loaded NPs with no irradiation or external magnetic field; d) in the presence of unloaded NPs under irradiation; e) in the presence of DOX-loaded NPs upon irradiation; f) in the presence of unloaded NPs and under irradiation and external magnetic field; g) in the presence of the DOX-loaded NPs under irradiation, and external magnetic field; h) in the presence of free DOX (18.2 μM). C) Monitoring the time-dependent HeLa tumor growth in mice: a) In the presence of unloaded NPs and under external magnetic field; b) tumor treated with PBS buffer; c) tumor treated with PBS buffer and laser irradiation (30 min, $\lambda = 808$ nm, power 3 $W cm^{-2}$); d) in the presence of DOX-loaded NPs under external magnetic field; e) in the presence of free DOX; f) in the presence of DOX-loaded NPs under irradiation; g) in the presence of unloaded NPs under irradiation and external magnetic field; h) in the presence of DOX-loaded NPs under irradiation and external magnetic field (one DOX dose); i) in the presence of DOX-loaded NPs under irradiation and external magnetic field (two DOX doses, the arrow indicates the time for injection of the second dose). Adapted with permission from Ref. [50]. Copyright 2014 American Chemical Society.

cancer cells[50] (Figure 5). Au NPs were deposited on octahedral Fe_3O_4 magnetic NPs, and the core–shell Fe_3O_4@Au NPs were coated with a SiO_2 layer that was further modified with an aminopropyltriethoxysilane layer (Figure 5A). The resulting nanoparticles were further functionalized with a maleimide layer. DOX was loaded in the pores of the mesoporous SiO_2 layer, and the drug was trapped in the pores by the covalent linkage of a thiolated nucleic acid duplex structure to the maleimide functionalities. The resulting drug-loaded NPs were incorporated into HeLa cancer cells, and the modified NPs acted as thermosensitive carriers for the release of the drug. Irradiation of the HeLa cells, which included the NPs, with a laser ($\lambda = 808$ nm) resulted in the localized heating of the NPs, leading to the dissociation of the duplex-DNA capping units, thus unlocking the pores and releasing the drug. Magnetic localization of the functionalized NPs and the light-induced thermal release of the drug led to a residual cell viability of ca. 34% after two hours of magnetic attraction of the NPs, followed by ten minutes of laser irradiation, whereas control experiments showed substantially higher cell viabilities (Figure 5B). Similarly, nude mice infected by HeLa tumors were subjected to intravenous (IV) injection of the DOX-loaded functionalized NPs. Thermoresponsive drug-loaded NPs were attracted to the tumor site by an external magnet (for 30 min), followed by the irradiation of the tumor ($\lambda = 808$ nm, laser power 3 $W cm^{-2}$, for 30 min). The effect of the thermal release of the drug on the growth of the tumor was then physically monitored. It has been demonstrated that the growth of the tumors was significantly inhibited by the magnetic-field/thermally activated drug-loaded NPs, as compared to control systems that did not release the drug (Figure 5C). It was also demonstrated that the dose of the IV-injected functionalized NPs, affected the extent of inhibition of the tumor growth.

The formation of stimuli-responsive supramolecular base-specific DNA nanostructures provides a versatile means to cap and release the loads entrapped in MP SiO_2 NPs. Cytosine-rich single-stranded nucleic acid self-assembles at acidic pH into the i-motif structure. Accordingly, MP SiO_2 NPs were functionalized with the C-rich nucleic acid **7**, and the pores were loaded with RhB at neutral pH. Subjecting the loaded NPs to pH 5.0 assembled the bulky i-motif structures that capped the pores[51] (Figure 6A). Treatment of the NPs at pH 8.0 separated the i-motif caps into random coil strands leading to the release of RhB from the pores (Figure 6B). By cyclic changing of the pH between the values pH 8.0 and pH 5.0, the ON/OFF switching of the release of RhB from the pores was demonstrated (Figure 6B, inset). In a related study,[52] MP SiO_2 NPs were functionalized with the nucleic acid **8**. Au NPs were modified with the C-rich nucleic acid **9** that is partially complementary to **8**. RhB was loaded in the **8**-functionalized MP SiO_2 NPs, and the hybridization of the **9**-modified Au NPs with the strand **8** yielded duplex structures in which the Au NPs capped the pores. Under acidic conditions, the strand **9** reconfigured to the i-motif structure, resulting in the separation of the Au NPs caps and the release of RhB from the pores (Figure 6C and D). By the cyclic switching of the system between pH 5.0 and pH 8.0, the system was switched between ON and OFF releasing states (Figure 6D, inset). The pH-stimulated release of loads from MP SiO_2 NPs is important because the pH of cancer cells is acidic as compared to normal cells. Accordingly, the targeted controlled release of chemotherapeutic drugs in cancer cells may be envisaged.

G-quadruplex structures represent a further supramolecular assembly of nucleic acid strands. The G-quadruplexes are stabilized by K^+ ions, and K^+-stabilized G-quadruplexes provide bulky nanostructures for capping loads in MP SiO_2 NPs. Figure 7A depicts the use of G-quadruplex as a stimuli-responsive cap for the controlled release of the RhB load.[53] The MP SiO_2 NPs were modified with the thiolated G-rich nucleic acid **10** and subsequently loaded with RhB. In the presence of K^+ ions, the strands **10** were reconfigured into the K^+-stabilized G-quadruplex that capped the pores. In the presence of kryptofix[2.2.2], the stabilizing K^+ was eliminated

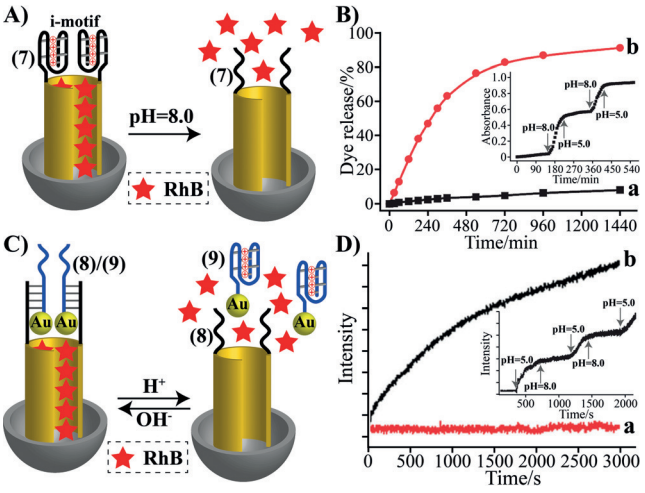

Figure 6. pH-Stimulated release of loads from pH-sensitive DNA-capped MP SiO_2 NPs: A) i-motif locked, dye-loaded MP SiO_2 NPs being unlocked by the separation of the i-motif caps at pH 8.0. B) Time-dependent fluorescence changes upon the pH-stimulated unlocking of the pores, and the release of the RhB loads: a) Pores are capped by the i-motif units, pH 5.0; b) pores are unlocked at pH 8.0. Inset: Switchable locking/unlocking of the pores and the controlled release of the dye at pH 5.0 and 8.0, respectively. Adapted with permission from Ref. [51]. Copyright 2011 Oxford University Press. C) The use of pH-responsive duplex DNA nanostructures functionalized with Au NPs as capping units, for the entrapment of RhB loads in MP SiO_2 NPs. The pH-stimulated unlocking of the pores and the release of RhB is stimulated by the separation of the i-motif-functionalized Au NPs from the capping units (pH 5.0). D) Time-dependent release of the dye, when: a) The pores are capped by duplex DNA nanostructures functionalized with Au NPs, pH 8.0; b) pores are unlocked at pH 5.0. Inset: Switchable locking/unlocking of the pores. Adapted with permission from Ref. [52]. Copyright 2011 Royal Society of Chemistry.

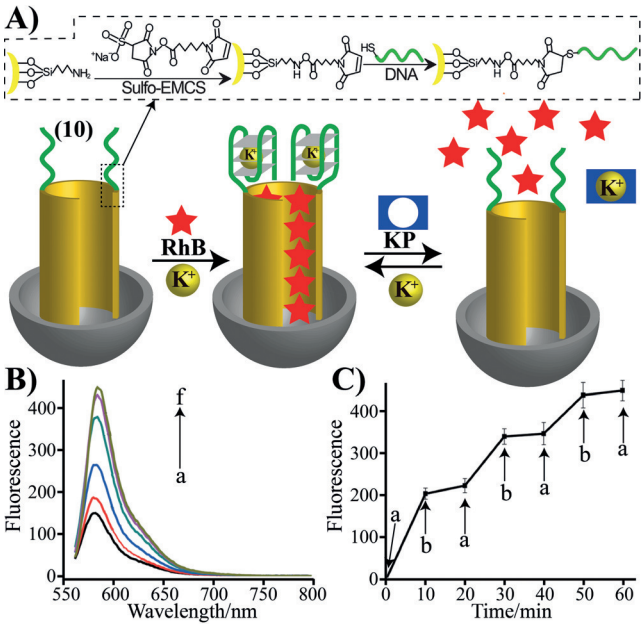

Figure 7. A) Synthesis of RhB-loaded MP SiO_2 NPs capped by K^+-ion-stabilized G-quadruplex units. Unlocking of the pores and release of RhB is achieved by kryptofix[2.2.2]-induced dissociation of the G-quadruplexes, by elimination of the K^+ ions. The release of RhB is switched ON and OFF by the cyclic treatment of the NPs with kryptofix[2.2.2] or K^+-ions, respectively. B) Fluorescence spectra of RhB released from the MP SiO_2 NPs (after a fixed time of 1 h), upon treatment with different concentrations of kryptofix[2.2.2]: a) 0 mM; b) 0.5 mM; c) 1 mM; d) 5 mM; e) 10 mM; f) 50 mM. C) Switchable and cyclic ON/OFF release of RhB from the G-quadruplex-capped pores upon treatment with: a) kryptofix[2.2.2]; b) K^+-ions. Adapted with permission from Ref. [53]. Copyright 2014 Wiley-VCH.

from the G-quadruplex units, resulting in the release of RhB loads (Figure 7B). By stepwise treatment of the system with K^+ ions and kryptofix[2.2.2], the NPs were switched between locked and unlocked states, respectively (Figure 7C). Many other nucleic acid strands in the presence of appropriate ligands form K^+-stabilized G-quadruplex aptamer–ligand complexes, e.g., the aptamer–thrombin complex. These complexes have been applied as locks of MP SiO_2 NPs, and these were similarly unlocked by the addition of kryptofix[2.2.2]. A different approach to unlock the pores by means of G-quadruplex units is exemplified in Figure 8A. The MP SiO_2 NPs were functionalized with the nucleic acid **11**, loaded with different guests, and caged in the pores by the hybrid duplexes between **12** and **11** acting as caps. The nucleic acid **12** was engineered to include a G-rich sequence that is caged in the duplex structures. In the presence of K^+ ions, the formation of the K^+-stabilized G-quadruplex separates the duplex, leading to the release of the loads.[53] Specifically, the chemotherapeutic drug doxorubicin (DOX) was loaded in the **11**/**12** duplex-capped NPs, and subsequently released from the pores by the K^+-ion-triggered dissociation of the G-quadruplex (Figure 8B and C). The cytotoxicity of the DOX-loaded NPs on normal breast epithelial cells (MCF-10a) and breast cancer cells (MDA-MB-231) was examined using the intracellular K^+-ion levels as unlocking triggers. It was found that although after an incubation time of 18 h only ca. 40% of the normal cells were killed, a 70% death of the cancer cells was observed under similar conditions (Figure 8D). The higher cytotoxic effect of DOX-loaded NPs on the cancer cells was attributed to the enhanced endocytosis of the NPs into these cells.[53]

A further supramolecular DNA nanostructure that was used as stimuli-responsive cap for the controlled release of chemotherapeutic drugs from MP SiO_2 NPs has involved intercalator-stabilized adenosine quadruplexes.[54] This has been demonstrated with the loading of the NPs with the indocyanine green (ICG), a near-infrared (NIR)-responsive chromophore, and with the coralyne alkaloid, known for its chemotherapeutic activity. The pores were capped by further intercalation of coralyne units into adenosine quadruplex units associated with poly(A). The localized heating of the caps with NIR excitation of ICG or the pH-stimulated dissociation of the A-quadruplexes released the coralyne drug (Figure 9A). The release rates of coralyne at different pH values, and upon NIR heating of the NPs, are depicted in Figure 9B and C. The potential therapeutic use of these chemothermal NIR-responsive NPs was demonstrated by the incorporation of the NPs into HepG2 cancer cells. It was reported that a cell culture, irradiated for 10 min with a NIR laser (780 nm, 2 $W cm^{-2}$), showed a cell viability of only

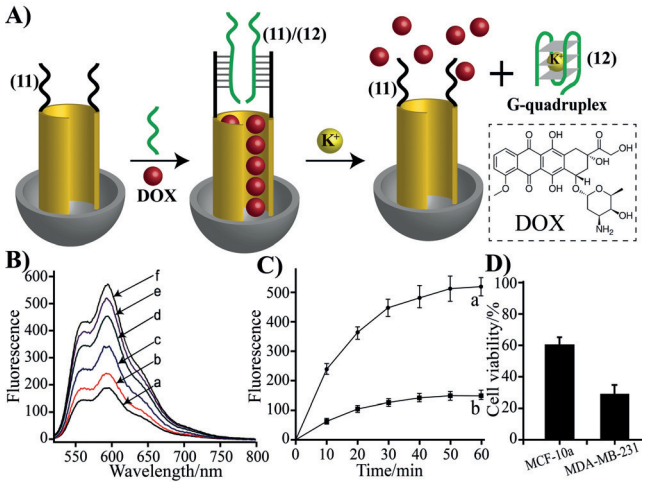

Figure 8. A) Synthesis of DOX-loaded MP SiO_2 NPs capped by duplex nucleic structures **11**/**12**, in which strand **12** includes a "caged" G-sequence capable of forming a G-quadruplex. In the presence of K^+ ions, the strand **12** is separated by the formation of a K^+-stabilized G-quadruplex, resulting in the release of DOX. B) Fluorescence spectra of the released DOX upon treatment of the DOX-loaded MP SiO_2 NPs with variable concentrations of K^+ ions for a fixed time interval of 1 h: a) 0 mM; b) 0.5 mM; c) 1 mM; d) 5 mM; e) 10 mM; f) 50 mM. C) Time-dependent fluorescence changes upon the release of DOX from the pores: a) In the presence of K^+ ions, 10 mM; b) in the absence of K^+ ions. D) The viability of MDA-MB-231 breast cancer cells and of normal MCF-10a breast cells after interaction with the **11**/**12**-locked DOX-loaded NPs for a time interval of 18 h. Adapted with permission from Ref. [53]. Copyright 2014 Wiley-VCH.

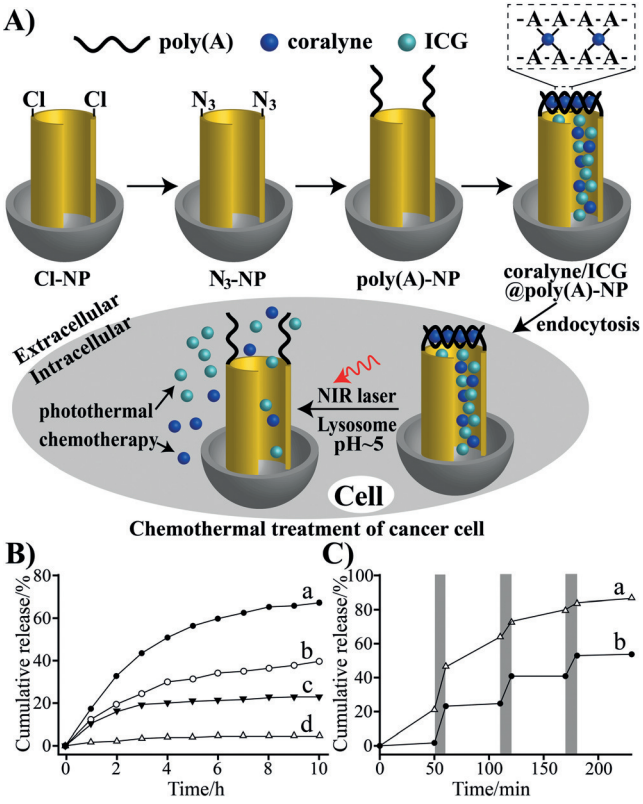

Figure 9. A) Preparation of MP SiO_2 NPs loaded with coralyne/indocyanine green (ICG) and capped by coralyne/poly(A) capping units, the chemothermal release of the coralyne drug using acidic environments, and the thermal dissociation of the capping units by irradiation of the ICG dye, which exhibits a high efficiency of NIR light-to-heat conversion. The Scheme depicts the effect of the intracellular acidic pH in cancer cells and of NIR laser irradiation on the release of the coralyne drug from the NPs. B) Time-dependent absorbance changes of released coralyne upon treatment of the coralyne/poly(A)-capped MP SiO_2 NPs with various pH environments: a) pH 4.0; b) pH 5.0; c) pH 6.0; d) pH 7.0. C) Switchable time-dependent absorbance changes corresponding to the release of coralyne upon unlocking coralyne/poly(A)-capped NPs in two different pH environments; a) pH 5.0; b) pH 7.0. The gray bars correspond to the time intervals in which the system is cooperatively thermally unlocked by the irradiation with a NIR laser ($\lambda = 780$ nm, power 2 $W cm^{-2}$). Adapted with permission from Ref. [54]. Copyright 2014 Royal Society of Chemistry.

23.8% after 48 h, whereas the nonirradiated cell culture showed a cell viability of ca. 60% after this time interval. The effective chemothermal release of coralyne suggests that local irradiation of the NIR chromophore could target the release of coralyne at tumors.

Aptamer-modified MP SiO_2 NPs were applied to cap the loads in MP SiO_2 NPs and to trigger the unlocking of the pores by formation of aptamer–ligand complexes.[55] For example, MP SiO_2 NPs have been functionalized with the nucleic acids **13** and **14** that are partially complementary to the ATP–aptamer sequence **15** (Figure 10A). The Ru^{II}-tris-bipyridine dye was loaded in the MP SiO_2 NPs and capped by the **13** + **14**/**15** duplex. In the presence of ATP as trigger, the energetically stabilized ATP–aptamer was formed, resulting in the unlocking of the pores and the release of the fluorescent load. A related method has applied Au nanoparticles modified with the anti-adenosine aptamer or the ATP aptamer units as capping units of the pores.[56] In the presence of adenosine or ATP, the selective ATP-triggered formation of the ATP–aptamer complex unlocked the pores, leading to the release of the loads entrapped in the pores. For example, Figure 10B depicts the unlocking of the RhB-loaded MP SiO_2 NPs using the formation of the adenosine–aptamer complex as pore-opening mechanism.[56a] The NPs were functionalized with the nucleic acid **16** and loaded with RhB. The pores were then capped by hybridization with the **17**-modified Au NPs to form the **16**/**17** duplex capping units. The nucleic acid **17** includes the anti-adenosine aptamer sequence, and this was partially "caged" in the duplex structure. In the presence of adenosine, the pores were unlocked by the dissociation of the caged aptamer sequence through formation of the adenosine–aptamer complex, leading to the release of RhB (Figure 10C). Similarly, the structural reconfiguration of hairpin structures capping the pores through the formation of an ATP–aptamer complex was used as a functional motive to unlock the pores.[45]

An approach to target the release of anticancer drugs into cancer cells has involved the implementation of a specific anticancer aptamer that locks the drugs in the porous materials, and unlocks the pores by the formation of specific aptamer–ligand complexes.[57] MP SiO_2 NPs were loaded with DOX and capped by the G-quadruplex-containing DNA **18** that forms duplex hybridization caps with the nucleic acid **19** strands associated with the NPs. The G-quadruplex domain I

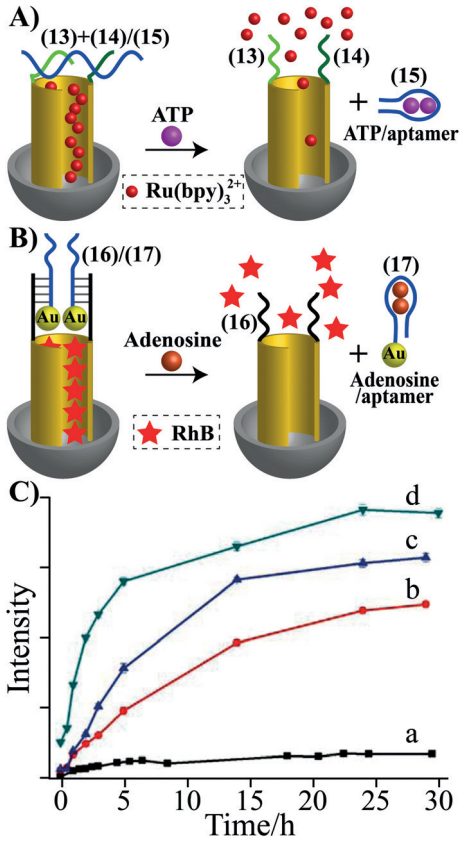

Figure 10. A) Preparation of a $Ru(bpy)_3^{2+}$-loaded MP SiO_2 NPs capped with the ATP aptamer strand **15**, bridging the nucleic acid scaffolds **13** and **14**. In the presence of ATP, the capping units are dissociated by forming the ATP–aptamer complex, resulting in the release of $Ru(bpy)_3^{2+}$. Adapted with permission from Ref. [55]. Copyright 2012 American Chemical Society. B) Preparation of RhB-loaded MP SiO_2 NPs capped by duplex DNA nanostructures, composed of **16**-linked SiO_2 NPs and **17**-functionalized Au NPs. The strand **17** includes the adenosine aptamer sequence. In the presence of adenosine, the adenosine/Au NP-functionalized aptamer complex separates, resulting in the unlocking of the pores, and the release of RhB. C) Time-dependent fluorescence changes upon the release of RhB from the MP SiO_2 NPs, in the presence of variable concentrations of adenosine: a) 0; b) 5 mM; c) 10 mM; d) 20 mM. Adapted with permission from Ref. [56a]. Copyright 2011 Royal Society of Chemistry.

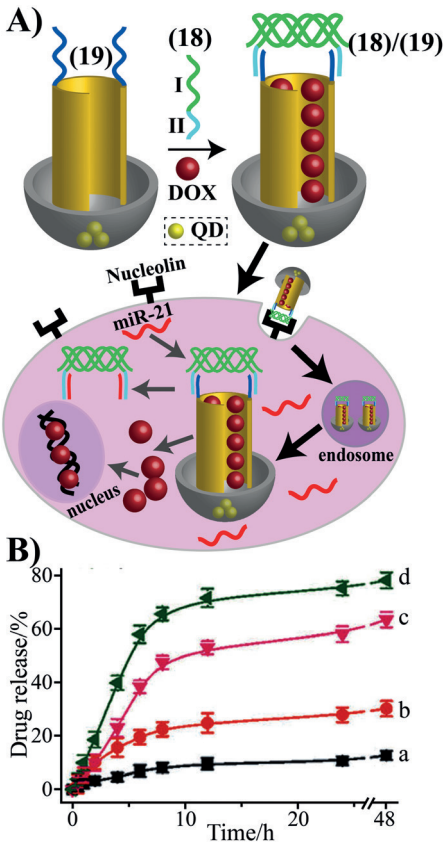

Figure 11. A) Synthesis of DOX-loaded MP SiO_2 NPs capped by the AS1411 aptamer as cancer-cell targeting unit. The aptamer domain I is extended by tethers II that exhibit complementarity to the strands **19**, associated with the NPs, and enhanced complementarity to the miR-21 cancer cell biomarker. The Scheme illustrates the "smart" mechanism for the release of DOX in cancer cells, in which the AS1411 aptamer targets the cancer cells and facilitates endocytosis of the NPs into the cells and the intracellular unlocking of the pores and release of the drug in the presence of miR-21. B) Time-dependent fluorescence changes upon the in vitro release of DOX from the AS1411 aptamer-capped MP SiO_2 NPs in the presence of variable ratios of miR-21:complex **18**/**19**: a) 0; b) 1; c) 2; d) 3. Adapted with permission from Ref. [57]. Copyright 2014 Wiley-VCH.

of **18** corresponds to the aptamer sequence that binds to the AS1411 receptor sites associated with the cancer cells, whereas domain II is complementary to the miR-21, that is a biomarker for the cancer cell. The aptamer site provides the targeting element for the association and incorporation of the NPs into the cancer cells. The secondary miR-21 displacement of the caps proceeding in the cell unlocked the pores and led to the release of the drug (Figure 11 A). The release of the drug was controlled by the concentrations of the miR-21 biomarker (Figure 11 B). A related system has implemented strontium hydroxyapatite as porous material for drug delivery and imaging of cancer cells.[58] In this system, DOX was loaded in the strontium hydroxyapatite pores, and the pores were capped by the anti-AS1411 receptor aptamer units. The resulting hybrid-capped material was targeted to the cancer cells (MCF-7), and unlocking of the pores by the association of the aptamer to the receptor sites released the drug.

Catalytic nucleic acids, DNAzymes, have been used to lock and unlock substrate-loaded MP SiO_2 NPs. Figure 12 A exemplifies the capping of substrate-loaded MP SiO_2 NPs with sequence-specific metal-ion-dependent DNAzymes and the selective release of the entrapped substrate by the activation of the DNAzymes in the presence of the respective ions.[59] The MP SiO_2 NPs were modified with the ribonucleobase-containing nucleic acid **20**, acting as substrate for either the Mg^{2+}-dependent or the Zn^{2+}-dependent DNAzyme. One group of NPs was loaded with methylene blue (MB^+) and capped with the Mg^{2+}-dependent DNAzyme sequence **21**. The second group of NPs was loaded with thionine (Th^+) and capped with the Zn^{2+}-dependent DNAzyme sequence **22**. In the presence of Mg^{2+} or Zn^{2+} ions, the respective DNAzyme-capped NP-loaded systems were activated, resulting in the release of MB^+ (Figure 12 B) or Th^+ (Figure 12 C). Selectivity toward unlocking of the pores by the specific cofactor ions, which activates the DNAzyme, was

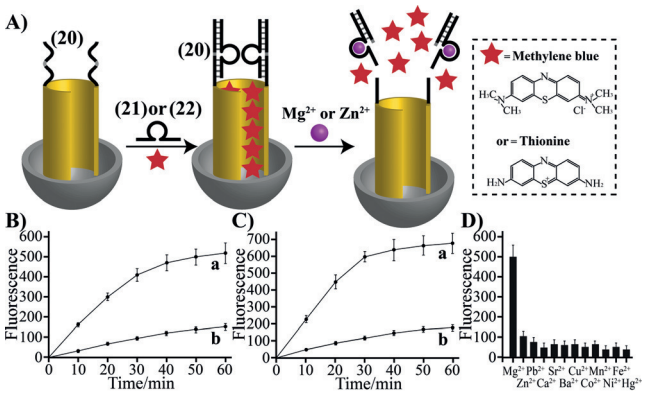

Figure 12. A) Loading of MP SiO_2 NPs with MB^+ or Th^+, and capping of the pores with the respective metal-ion-dependent DNAzyme/substrate sequences, in which the metal-dependent DNAzymes correspond to the Mg^{2+}- or the Zn^{2+}-dependent DNAzymes, and the respective substrates are covalently linked to the NPs. Unlocking of the pores proceeds by activation of the DNAzymes by the respective ions that result in the cleavage of the substrates, and the release of capping units. B) Time-dependent fluorescence changes upon the Mg^{2+}-triggered release of MB^+ from the Mg^{2+}-dependent DNAzyme/substrate-capped MP SiO_2 NPs: a) With Mg^{2+}, 10 mM; b) in the absence of Mg^{2+} ions. C) Time-dependent fluorescence changes upon the Zn^{2+}-triggered release of Th^+ from the Zn^{2+}-dependent DNAzyme/substrate-capped MP SiO_2 NPs: a) With Zn^{2+}, 5 mM; b) in the absence of Zn^{2+} ions. D) Results demonstrating the selective release of MB^+ from the Mg^{2+}-dependent DNAzyme/substrate-capped MP SiO_2 NPs in the presence of Mg^{2+} ions. Adapted with permission from Ref. [59]. Copyright 2013 American Chemical Society.

demonstrated. Figure 12D shows the ion selectivity of the Mg^{2+}-dependent DNAzyme sequence for the release of MB^+ in the presence of added Mg^{2+} ions. Similarly, treatment of the NPs mixture with Mg^{2+} and Zn^{2+} ions unlocked both kinds of NPs, resulting in the release of MB^+ and Th^+. The DNAzyme-stimulated unlocking of substrate-loaded MP SiO_2 NPs has been extended by developing pH-programmable stimuli-responsive NPs, being activated by different metal ions[60] (Figure 13A). The Mg^{2+}-dependent DNA reveals high activity at pH 7.2 and is inactive at pH 5.2. In turn, the UO_2^{2+}-dependent DNAzyme is inactive at pH 7.2, yet it reveals high activity at pH 5.2. At pH 6.0, both of the DNAzymes exhibit moderate activity. Accordingly, two classes of DNAzyme-capped MP SiO_2 NPs were prepared. MP SiO_2 NPs were functionalized with the ribonucleic acid **23** acting as substrate for the Mg^{2+}- or UO_2^{2+}-dependent DNAzymes. One class of NPs (class I) was loaded with MB^+ and capped with the Mg^{2+}-dependent DNAzyme sequence **24**. The second class (class II) of MP SiO_2 NPs was loaded with Th^+ and capped with the UO_2^{2+}-dependent DNAzyme sequence **25** (Figure 13A). At pH 7.2 and in the presence of Mg^{2+} ions, the Mg^{2+}-dependent DNAzyme was activated and the NPs of class I were unlocked, resulting in the release of MB^+ (Figure 13B). In turn, treatment of the MP SiO_2 NPs of class II with UO_2^{2+} at pH 5.2, resulted in the selective unlocking of the NPs of class II, and the release of Th^+ (Figure 13C). Upon mixing the two classes of NPs and subjecting it to the mixture of the Mg^{2+}- and UO_2^{2+}-ions the release of the MB^+ and Th^+ load occurred. The different pH-dependence of the Mg^{2+}- and

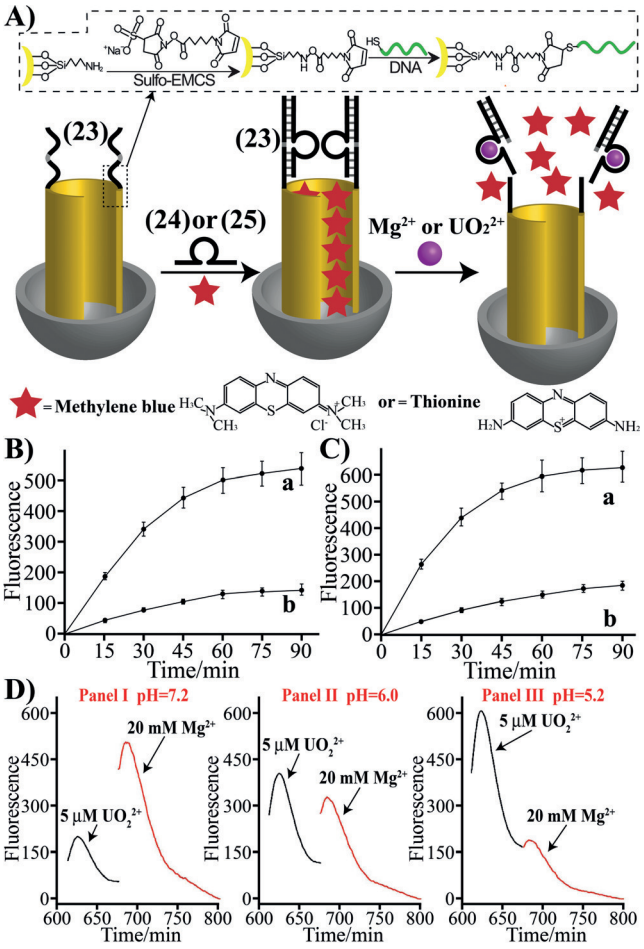

Figure 13. A) pH-Programmed release of loads (MB^+ or Th^+) from metal-ion-dependent DNAzyme/substrate-capped MP SiO_2 NPs (metal ions = Mg^{2+} and/or UO_2^{2+}). At pH 7.2 the Mg^{2+}-dependent DNAzyme is triggered-on, resulting in the release of MB^+, yet the UO_2^{2+}-dependent DNAzyme is inactive. At pH 5.2 only the UO_2^{2+}-dependent DNAzyme is active leading to the release of Th^+. At pH 6.0 the Mg^{2+}- and UO_2^{2+}-dependent DNAzymes reveal partial activity, resulting in the unlocking of both kinds of MP SiO_2 NPs. B) Time-dependent fluorescence changes upon the activation of the Mg^{2+}-dependent DNAzyme/substrate-capped NPs at pH 7.2 and the release of MB^+ loads in the presence of: a) Mg^{2+} 20 mM; b) without added Mg^{2+}. C) Time-dependent fluorescence changes upon the activation of the UO_2^{2+}-dependent DNAzyme/substrate-capped NPs at pH 5.2, and the release of Th^+ loads, in the presence of: a) UO_2^{2+}, 5 μM; b) without added UO_2^{2+}. D) pH-programmed logic activation of the mixture of MP SiO_2 NPs loaded with MB^+ or Th^+ and capped with the Mg^{2+}- or UO_2^{2+}-dependent DNAzyme/substrate units. Adapted with permission from Ref. [60]. Copyright 2014 Royal Society of Chemistry.

UO_2^{2+}-dependent DNAzymes allowed the pH-programmed release of the loads (Figure 13D); at pH 7.2 only the Mg^{2+}-dependent DNAzyme was activated and MB^+ was released, whereas at pH 5.2, only the UO_2^{2+}-dependent DNAzyme was activated and the release of Th^+ occurred. In turn, at pH 6.0, both of the DNAzymes were activated and the release of MB^+ and Th^+ proceeded. The programmed release of loads from the nucleic-acid-functionalized mesoporous NPs follows the basic concepts of logic-gate systems. Indeed, recent reports addressed the interplay between stimuli-responsive nucleic-

acid-functionalized MP SiO_2 NPs as load carriers and as functional components for logic gate operations.[61]

The catalytic properties of metal-ion-dependent DNAzymes were combined with the specific recognition functions of aptamers, to yield stimuli-responsive capped NPs, acting as sense-and-treat functional drug carrier.[59] It was reported that the separation of two metal-dependent subunits by a tandem nucleic acid insert, deactivates the DNAzyme catalytic functions in the presence of the appropriate cofactor metal ion, presumably due to the flexibility of the loop that prevents the stabilization of the DNAzyme structure. However, the rigidification of the flexible insert strand, e.g., by the formation of an aptamer–ligand complex, was found to reassemble the rigid structure of the DNAzyme loop that allows the reactivation of the catalytic properties of the DNAzyme[59] (Figure 14A). The allosteric activation of

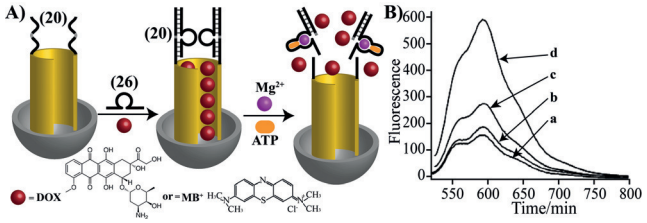

Figure 14. A) Preparation of MB^+ or DOX-loaded MP SiO_2 NPs caged by ATP-aptamer-modified Mg^{2+}-dependent DNAzyme/substrate capping units. Unlocking of the pores and the release of the loads are triggered by the cooperative activation of the DNAzyme in the presence of Mg^{2+} ions and ATP. B) Fluorescence spectra corresponding to the released DOX after a 1 h-treatment of the NPs with: a) No added Mg^{2+} ions and ATP; b) ATP, 100 μM; c) Mg^{2+}, 20 mM; d) Mg^{2+}, 20 mM and ATP, 100 μM. Adapted with permission from Ref. [59]. Copyright 2013 American Chemical Society.

a DNAzyme by an aptamer–ligand complex was demonstrated by loading the **20**-modified MP SiO_2 NPs with a model load substrate MB^+ or the anticancer drug DOX, and by capping the pores with the Mg^{2+}-dependent DNAzyme sequence **26** that includes the anti-ATP aptamer as functional insert sequence. In the presence of Mg^{2+} ions, the release of the loads was prohibited, due to the inactive conformation of the DNAzyme sequence. In the presence of Mg^{2+} ions and ATP, the formation of the ATP–aptamer complex rigidified the active loop structure of the Mg^{2+}-dependent DNAzyme, resulting in the release of the loads. Figure 14B exemplifies the enhanced release of DOX in the presence of the ATP and Mg^{2+} stimuli. The fact that ATP is overexpressed in cancer cells, due to their enhanced metabolism, suggests that the ATP–aptamer/DNAzyme capping units provide a "smart" unlocking mechanism for the specific release of the drug in cancer cells. That is, the ATP biomarker is sensed by the carrier nanoparticles and it preferentially activates the release of the drug in the cancer cells.

The metal-dependent DNAzymes are promising locks for the controlled release of drugs from the NPs. Different metal ions, e.g., Cu^{2+}, are overexpressed in cancer cells.[62] Accordingly, these ions could act as biomarkers for activating DNAzymes and releasing drug loads. Furthermore, because cancer cells exhibit increased acidity as compared to normal cells,[63] the pH-programming of metal-dependent DNAzymes for unlocking the pores could provide a mechanism for targeting the release of the drugs in cancer cells.

The optically (photonic) triggered unlocking of DNA-capped MP SiO_2 NPs provides a further means to stimulate the controlled release of loads from the NP.[64] For example, one method has utilized the use of photoisomerizable intercalators as a means to control the stability of duplex-DNA capping units (Figure 15A). *Trans*-azobenzene units are known to intercalate and stabilize duplex DNA structures. Photoisomerization of the *trans*-azobenzene units (UV light)

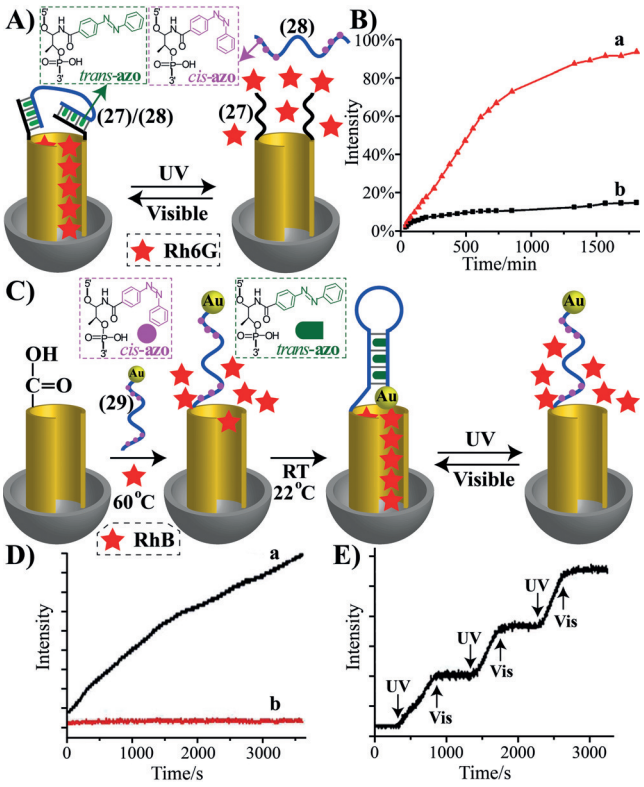

Figure 15. A) Synthesis of azobenzene photoresponsive DNA-capped Rh6G-loaded MP SiO_2 NPs. Photoisomerization of the caps unlocks the pores. B) Time-dependent release of Rh6G from the *trans*-azobenzene duplex-DNA-capped MP SiO_2 NPs upon: a) Photoisomerization of the *trans*-azobenzene units to *cis*-azobenzene; b) non-irradiated MP SiO_2 NPs. Adapted with permission from Ref. [64]. Copyright 2012 American Chemical Society. C) Synthesis of RhB-loaded photoresponsive hairpin DNA-capped MP SiO_2 NPs. The hairpin capping units are cooperatively stabilized by *trans*-azobenzene intercalator units. Photoisomerization of the *trans*-azobenzene units to *cis*-azobenzene separates the hairpin units, resulting in the unlocking of the pores and the release of RhB. By the reversible photoisomerization of the azobenzene units between the *trans*-azobenzene and *cis*-azobenzene, the cyclic closure and opening of the pores proceeds. D) Time-dependent fluorescence changes observed upon: a) Photoisomerization of the RhB-loaded *trans*-azobenzene-stabilized hairpin-capped MP SiO_2 NPs (UV light); b) non-irradiated NPs. E) Switchable ON/OFF release of RhB from the hairpin-locked RhB-loaded NPs, upon the cyclic UV-light-stimulated formation of *cis*-azobenzene units and visible-light-induced formation of *trans*-azobenzene units, respectively. Adapted with permission from Ref. [65]. Copyright 2012 Royal Society of Chemistry.

leads to the formation of *cis*-azobenzene isomers that lack binding affinity to duplex DNA. In turn, the reverse photoisomerization of the *cis*-azobenzene states to the *trans*-state configuration (visible light) restores the energetically stabilized duplex structures. Accordingly, the MP SiO_2 NPs were functionalized with the nucleic acid strands **27**, and these were loaded with rhodamine 6G (Rh6G). Subsequently, the loaded NPs were interacted with the *trans*-azobenzene-modified nucleic acid **28** that exhibits partial base complementarities to **27**. Hybridization of **28** with the **27** units and the cooperative stabilization of the duplex units by the *trans*-azobenzene units, led to the capping of the pores. The subsequent photoisomerization of the *trans*-azobenzene units to the *cis*-azobenzene state, destabilized the duplex capping units, resulting in the unlocking of the pores, and the release of Rh6G. Figure 15B depicts the photonically triggered release of Rh6G upon photoisomerization of the *trans*-azobenzene units to the *cis*-azobenzene state. A related system has applied MP SiO_2 NPs functionalized with a *trans*-azobenzene nucleic acid **29** and tethered to Au NPs.[65] The nucleic acid **29** includes internal self-complementarity that, in the presence of the *trans*-azobenzene units, cooperatively stabilizes a hairpin structure, in which the hairpin-functionalized Au NPs block the pores. To load the MP SiO_2 NPs, and to yield the photonically activated NPs, the NPs were heated to separate the hairpin structure and yield the open structure of the pores (Figure 15C). Subsequently, the NPs were loaded with RhB, and upon cooling the reconfiguration of the random coil structure of **29** to the energetically stabilized *trans*-azobenzene hairpin/Au NPs-locked pore structure occurred. The irradiation of the NPs with UV light transformed the *trans*-azobenzene stem-intercalated units into the *cis*-azobenzene photoisomer states, lacking affinity for the duplex stem domain. The removal of the stabilizing *trans*-azobenzene units from the hairpin stem domain weakened the hairpin structure, resulting in the unlocking of the pores and the release of RhB (Figure 15D). By the cyclic photoisomerization of the hairpin *trans*-azobenzene-functionalized **29**/Au NP caps between the *cis*-configuration (UV light) and *trans*-configuration (visible light), the release of RhB from the pores was switched between ON and OFF states, respectively (Figure 15E).

A different approach to photonically trigger the controlled release of loads entrapped in MP SiO_2 NPs has applied the photoinduced heterolytic cleavage of Malachite Green carbinol (MGCB) and the accompanying pH changes of the aqueous medium as a means to control the pH-driven locking/unlocking of functional DNA caps, which are associated with the NPs[66] (Figure 16A). MP SiO_2 NPs were modified with the cytosine-rich nucleic acid **30**, loaded with Ru^{II}-tris-bipyridine, and locked by acidification of the system (pH 5.0) through the formation of the bulky i-motif caps. The solution included the Malachite Green photoactive substrate, and irradiation of the system resulted in the heterolytic cleavage of the photoactive compound to yield OH^-. Neutralization of the system dissociated the i-motif caps, resulting in the release of the pore-entrapped substrate (Figure 16B).

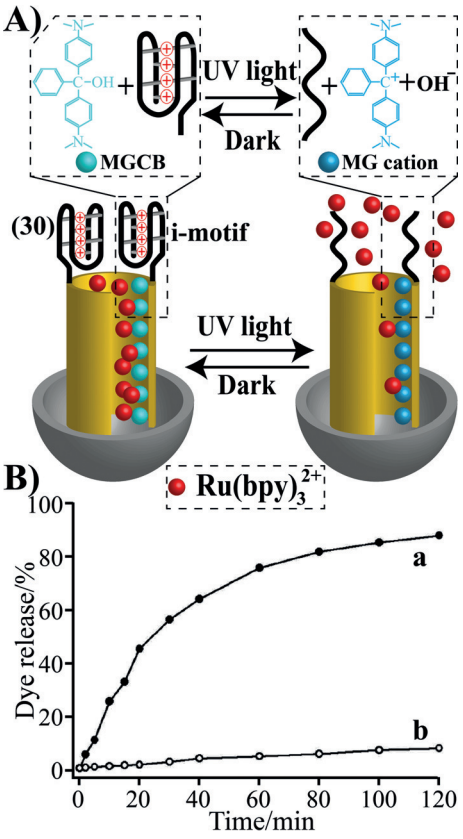

Figure 16. A) Photostimulated pH-induced release of $Ru(bpy)_3^{2+}$-loaded MP SiO_2 NPs capped by i-motif DNA units. The pores are co-loaded with $Ru(bpy)_3^{2+}$ and Malachite Green carbinol (MGCB) as photosensitive compound. UV irradiation of the Malachite Green results in its heterolytic cleavage of the photosensitizer, resulting in the neutralization of the system, and the separation of the i-motif caps and the release of $Ru(bpy)_3^{2+}$. B) Time-dependent fluorescence changes of released $Ru(bpy)_3^{2+}$ upon: a) UV irradiation of the MP SiO_2 NPs loaded with $Ru(bpy)_3^{2+}$/Malachite Green and capped by the i-motif units; b) non-irradiated NPs. Adapted with permission from Ref. [66]. Copyright 2012 Wiley-VCH.

A different approach to photonically trigger the release of loads from the MP SiO_2 NPs has involved the effect of photogenerated reactive oxygen intermediates on the unlocking of the pores[67] (Figure 17A). MP SiO_2 NPs were functionalized with the G-rich nucleic acids **31** and folic acid units. The pores of the NPs have been loaded with RhB or the anticancer drug DOX, and the pores were locked by self-assembly of the G-rich strand into G-quadruplexes. *Meso*-tetra(*N*-methyl-4-pyridinium)porphyrin was used as photosensitizer for the generation of reactive oxygen species (ROS) under irradiation. The folic acid residues associated with the NPs facilitated the targeting and permeation of the NPs into cancer cells. The photosensitizer-stimulated ROS degraded the G-rich strands, resulting in the unlocking of the pores. Figure 17B depicts the release of RhB from the pores upon irradiation of the NPs. The DOX-loaded MP SiO_2 NPs were then incorporated into HepG2 cells, and the cell viability upon irradiation of the cells in the presence of porphyrin-modified MP SiO_2 NPs, and in the absence or presence of DOX, was examined (Figure 17C). While in the absence of

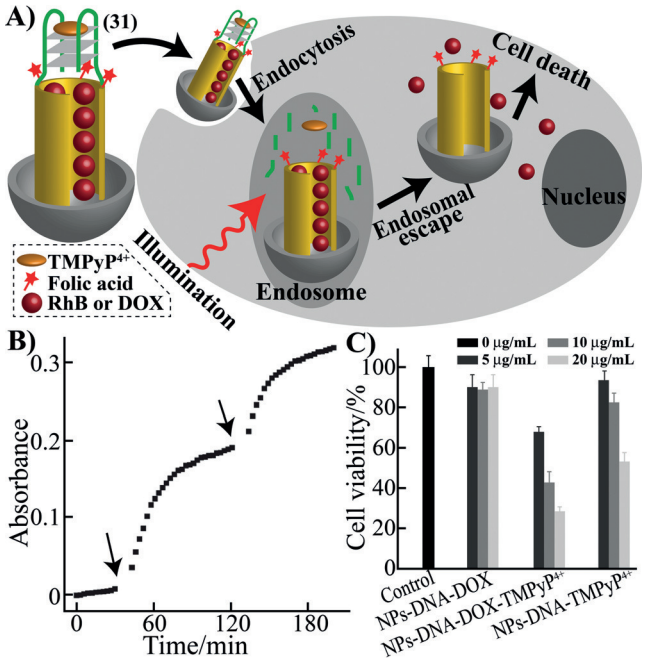

Figure 17. A) Synthesis of RhB- or DOX-loaded MP SiO_2 NPs capped by G-quadruplex units and the *meso*-tetra(*N*-methyl-4-pyridinium)porphyrin ($TMPyP^{4+}$) photosensitizer. The surface of MP SiO_2 NPs is modified with folic acid units acting as targeting ligands to folic acid receptors associated with cancer cells. The unlocking mechanism involves the photosensitizer-induced generation of $^1O_2$ that degrades the G-quadruplex caps, leading to the release of the loads. B) Time-dependent absorbance changes due to the release of RhB upon the photosensitized generation of $^1O_2$ (arrows indicate the light-induced triggering events that yield $^1O_2$). C) HepG2 cancer cell viability in the presence of different concentrations of DOX-loaded folic-acid-functionalized MP SiO_2 NPs capped with $TMPyP^{4+}$-G/quadruplex units. Adapted with permission from Ref. [67]. Copyright 2013 Wiley-VCH.

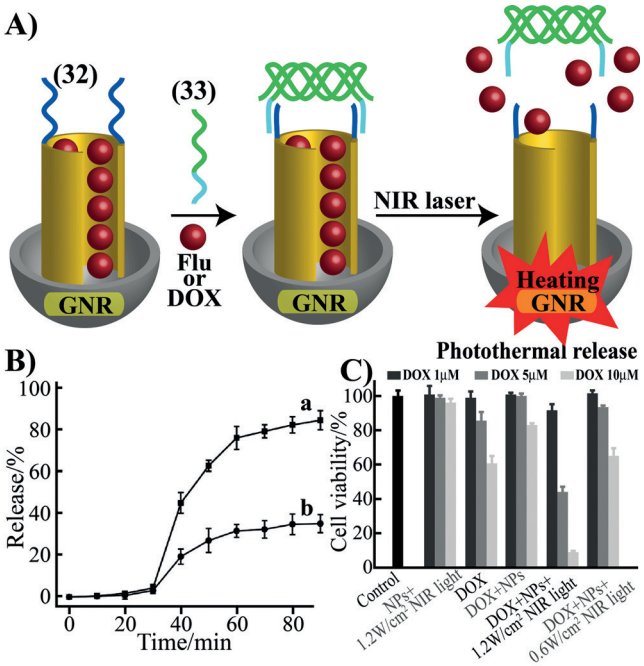

Figure 18. A) Thermally triggered unlocking of MP SiO_2 NPs-coated Au nanorods, loaded with a fluorescence dye or DOX, and capped with the AS1411 anticancer cell aptamer. The unlocking of the pores is achieved by NIR laser irradiation of the plasmonic nanorods, which results in localized heating of the NPs. B) Time-dependent fluorescence changes resulting in the release of the fluorescein load upon irradiation of the NPs with different NIR laser powers (808 nm): a) 1.2 $W cm^{-2}$; b) 0.6 $W cm^{-2}$. C) Cell viability of MCF-7 human breast cancer cells treated with variable doses of DOX-loaded MP SiO_2 NPs coated with Au nanorods and capped by the AS1411 aptamer, and the respective control systems. Release of DOX is triggered by irradiation of the NP-functionalized cells with a NIR laser (808 nm) for 10 min. Adapted with permission from Ref. [68]. Copyright 2012 Wiley-VCH.

DOX, the photosensitized formation of ROS products resulted in cell death, the photosensitized unlocking of the DOX-loaded NPs had an impressive cooperative effect in enhancing cell death. For example, the cells treated with 20 $\mu g mL^{-1}$ of unloaded SiO_2 NPs showed a cell viability of ca. 52% after 120 s of irradiation, whereas the DOX-loaded NPs showed a cell viability of ca. 29% under the same conditions.

A further method for the light-induced release of loads from MP SiO_2 NPs involves plasmonic heating of the porous NPs by Au nanorods (GNR), using NIR-laser irradiation.[68] Au nanorods were coated with MP SiO_2 NPs and the nanoparticles were modified with the nucleic acid **32**, which acted as a scaffold for hybridization with the anticancer guanine-rich AS1411 aptamer **33** (Figure 18A). The **32**-functionalized MP SiO_2 NPs coating the Au nanorods were loaded with fluoresceine (Flu) as model-load or with DOX as anticancer drug. The pores were then capped by hybridization with the AS1411 aptamer **33**, which was extended by tethers complementary to the nucleic acid scaffold **32** and linked to the NPs. The irradiation of the NPs with an 808 nm NIR laser resulted in the plasmonic heating of the NPs, the dissociation of the AS1411 aptamer units, and the release of the loads. Figure 18B depicts the time-dependent release of the fluorescein model-load upon irradiation of the NPs at different power intensities of the laser light source. The DOX-loaded NPs capped with the AS1411 aptamer were then incorporated into human breast cancer cells MCF-7. The AS1411 anticancer aptamer units targeted the NPs to the cancer cells and facilitated their incorporation in the cells. Irradiation of the NPs with an 808 nm laser resulted in the plasmonic thermal unlocking of the pores and the release of the chemotherapeutic drug. Impressive cytotoxicity toward the cancer cells was observed (Figure 18C). For example, the thermal NIR-laser-stimulated release of DOX (laser power 1.2 $W cm^{-2}$ irradiation for 10 min) resulted in a cell viability of less than 10%, whereas the cell assay heated without the DOX load, or unheated DOX-loaded NPs, showed cell viabilities above 60%. Other nucleic acid structures have been similarly used to lock loads in MP SiO_2 NPs coating Au nanorods, and the resulting nanocarriers were unlocked by the NIR-irradiated heating of the assemblies.[69]

3. Stimuli-Responsive Microcapsules for Controlled Release

Capsules in the nanometer or micrometer size provide an interesting system for the incorporation of payloads.[70] Different applications of substrate-loaded capsules have been suggested, including the carrying and release of drugs,[71] as imaging[72] or sensing agents,[73] and their use as sense-and-treat systems,[74] or as catalyst carriers.[75] Various methods to prepare micro-/nanocapsules have been suggested.[76] These usually involve the use of colloidal particles as core template for the deposition of layers or films (e.g., polystyrene, $CaCO_3$, SiO_2). Affinity binding interactions between the deposited layers[77] or covalent-bond-bridging of the deposited layers generate the shells of the capsules,[78] and the subsequent dissolution of the core template yields the capsules. By the co-immobilization of guest molecules with the core material, the resulting capsules are loaded with the guest compound. The nature of the shell materials, the number of deposited layers, and the interactions or bonds participating in the shell formation, control the size, rigidity, permeability, and stability of the capsules.[79] For example, the layer-by-layer deposition of polyelectrolyte layers,[80] e.g., polystyrene sulfonate/polyallylamine hydrochloride or disulfide-bridged multilayers,[81] have been used to assemble capsules. Different stimuli-responsive shells that enable the degradation of the capsule shells and the release of the loads have been reported.[82] These include the enzymatic digestion of poly(L-lysine)/poly(L-glutamic acid),[83] the biodegradation of disulfide-bridged shells by the reduction of bonds with thiols,[84] and the engineering of pH-responsive shells.[85] Also, the incorporation of metal nanoparticles, e.g., Au nanorods or magnetic nanoparticles into the capsules, enables the thermal cleavage of capsules by NIR-laser irradiation.[86] Indeed, stimuli-responsive microcapsules have been used as carriers for the controlled release of drugs such as insulin[87] or the anticancer drug DOX.[88] Several Review articles have addressed the recent advances in the preparation and applications of micro-/nanocapsules.[89]

The specific recognition properties or the electrical charge of biomolecules make biomaterials ideal components for the construction of microcapsules. Indeed, receptor–ligand complexes[90] as well as electrostatic binding with the negatively charged DNA polyelectrolyte have been implemented to construct microcapsules.[91] Furthermore, the information encoded in DNA strands might be used to design stimuli-responsive microcapsules that act as microcarriers of loads, being released upon the triggered dissociation of the capsules. Indeed, different approaches to dissociate DNA-based microcapsules, and release the loads, have been reported in recent years.

The synthesis of degradable all-DNA microcapsules is exemplified in Figure 19 A.[92] Positively charged amine-functionalized SiO_2 microparticles were coated with the poly-T_{30} oligonucleotide, and these base layers were hybridized with the triblock oligonucleotide $A_{15}X_{15}G_{15}$ that acted as scaffold for the subsequent hybridization with the triblock oligonucleotide $T_{15}X_{15}C_{15}$. By the subsequent alternate stepwise interaction of the bilayer structure with the two triblock

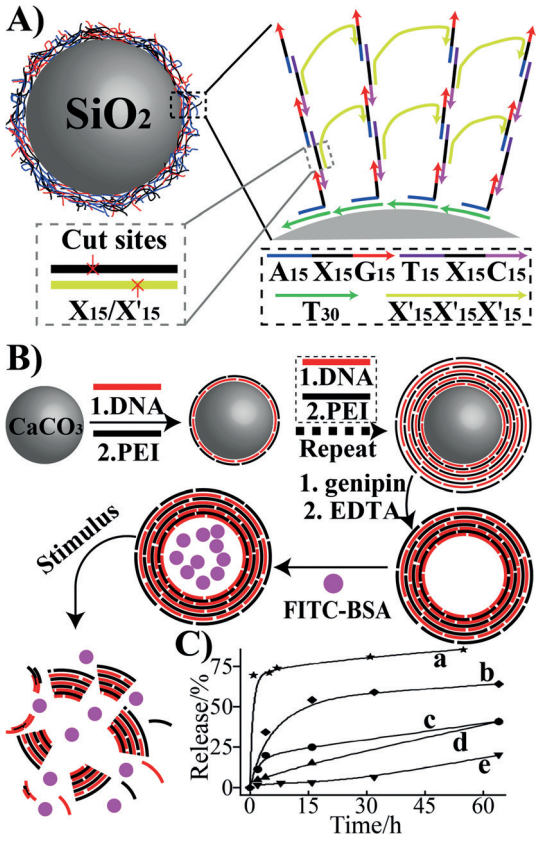

Figure 19. A) Synthesis of all-DNA capsules consisting of nucleic acid cross-linked layers. The cleavage of the cross-linking units by a nicking enzyme dissociates the capsules. Adapted with permission from Ref. [92]. Copyright 2009 Wiley-VCH. B) Assembly of DNA-based capsules by the layer-by-layer deposition of polyethyleneimine/DNA polyelectrolyte layers, followed by dissolution of the $CaCO_3$ core (with EDTA). The capsules were loaded with FITC-labeled BSA, and the release of the load was triggered by T7 exonuclease, pH 10.1, or NaCl (1 M or 0.5 M). C) Time-dependent release of FITC-labeled BSA from the capsules upon treatment with: a) T7 exonuclease enzyme; b) pH 10.1; c) 1 M NaCl; d) 0.5 M NaCl; e) PBS buffer solution. Adapted with permission from Ref. [93]. Copyright 2014 Royal Society of Chemistry.

oligonucleotides $A_{15}X_{15}G_{15}$ and $T_{15}X_{15}C_{15}$, a stepwise construction of DNA chains on the core microparticles was generated. The subsequent cross-linking of the chains by the triblock oligonucleotide $X'_{15}X'_{15}X'_{15}$ leads to the formation of the layer DNA film, which is cross-linked by the hybrid domains X/X′. The dissolution of the core SiO_2 microparticles (2 M HF and 8 M NH_4F, pH 5.0) resulted in hollow DNA capsules. The domains X/X′ were designed, however, to include the specific sequence to be cleaved by the *Eco*RI endonuclease. Accordingly, the as-prepared microcapsules were degraded in the presence of the endonuclease. A related study has implemented $CaCO_3$ microparticles as the core material for the generation of the microcapsules by stepwise coating of the cores with the negatively charged DNA polyelectrolyte and the positively charged polyethylenimine (PEI).[93] By subsequent rigidification of the multilayer structure with genipin and the subsequent EDTA-stimulated dissolution of the core particles, hollow microcapsules were

formed and loaded with the fluorophore fluorescein isothiocyanate bovine serum albumin (FITC-BSA; Figure 19B). The stabilized wall of the microcapsule could then be degraded either by enzymatic digestion of the DNA component using T7 exonuclease, by subjecting the capsules to pH 10.1 which neutralizes the positive charges of the PEI units, or by applying a high salt concentration (NaCl 1M) which weakens the electrostatic binding interaction between the polyelectrolyte layers. The different triggers that degraded the microcapsules resulted in the release of FITC-BSA (Figure 19C). This approach was further developed by constructing layer-by-layer hybridized peptide nucleic acids as DNA shells of microcapsules, and the cleavage of the shells was achieved by applying a nuclease or protease as catalyst for degradation of the shells.[94]

A different approach to unlock DNA-functionalized microcapsules involved the incorporation of a sequence-specific aptamer into the microcapsules and the opening of the capsules by the formation of aptamer–ligand complexes[95] (Figure 20). $CaCO_3$ microparticles were coated with the anti-

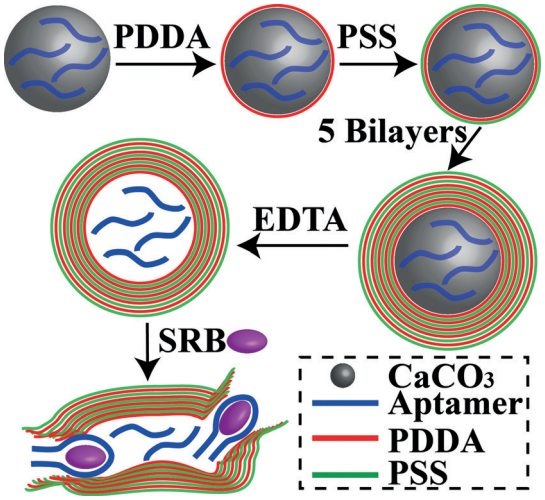

Figure 20. Trapping of aptamer loads in microcapsules assembled by a layer-by-layer deposition process of negative and positive polyelectrolyte layer. The capsules are dissociated by the formation of aptamer–ligand complexes. Adapted with permission from Ref. [95]. Copyright 2013 American Chemical Society.

sulforhodamine B aptamer, and these acted as cores for the layer-by-layer deposition of the two polyelectrolytes poly(diallyldimethylammonium chloride) (PDDA) and poly(styrene sulfonate) (PSS), respectively. The dissolution of the cores by EDTA led to the formation of the aptamer-loaded microcapsules. The intershell diffusion of sulforhodamine B (SRB) resulted in the formation of the respective ligand–aptamer complex that ruptured the microcapsule structure, resulting in the release of the SRB–aptamer complex.

A different paradigm to generate all-DNA capsules has involved the design of a photosensitive three-point star-shaped DNA unit that self-assembled into a polyhedron structure (fullerene-like structure), acting as light-responsive nanocapsule[96] (Figure 21A). A DNA-scaffold L was hybrid-

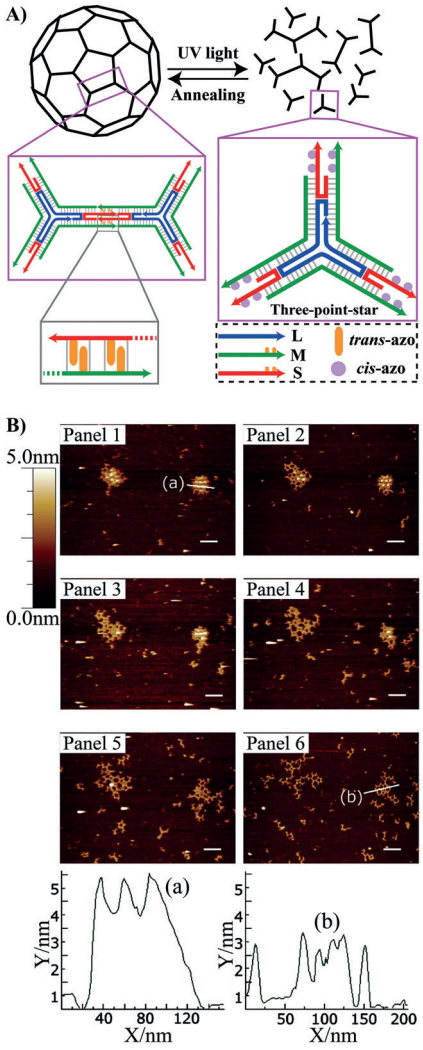

Figure 21. A) Self-assembly of an all-DNA polyhedron (fullerene-like) nanostructure using *trans*-azobenzene-functionalized nucleic acid toeholds associated with a three-point-star Y-shaped DNA as building unit. The photoisomerizable *trans*-azobenzene units cooperatively stabilize the cross-linking of the three-point-star Y-shaped units. The capsules are separated by photoinduced isomerization of the *trans*-azobenzene units to *cis*-azobenzene. B) AFM images following the capsule nanostructures at different time intervals of photoisomerization of the *trans* units to *cis* units: Panel 1: Before UV irradiation; panel 2: 30 s after UV irradiation; panel 3: 1 min 6 s after UV irradiation; panel 4: 2 min 12 s after UV irradiation; panel 5: 5 min after UV irradiation; panel 6: 9 min 58 s after UV irradiation. Bottom: Cross section analysis of: The capsules a) before and b) after photoisomerization. Adapted with permission from Ref. [96]. Copyright 2010 American Chemical Society.

ized with the two *trans*-azobenzene-modified strands, S and M, to yield a three-point star-shaped nanostructure that included at each arm single-stranded toeholds associated with the S and M strands that exhibit self-complementarity. Annealing of the three-point-star units resulted in the *trans*-azobenzene-stabilized polyhedra as a result of interhybridization of the "star" subunits. Photoinduced isomerization of the *trans*-azobenzene to the *cis*-azobenzene isomer state, which lacks affinity toward the duplex DNA bridges, resulted

in the destabilization of the interstar-linking units, leading to the separation of the nanocapsules (Figure 21 B).

A further approach to assemble photoresponsive all-DNA nanocapsules has involved the assembly of programmed origami DNA-based square-bipyramidal DNA nanocapsules[97] (Figure 22 A). A square-bipyramid origami nanostructure composed of fused subunits A and B was constructed. One of the edges of the two square origami faces of the units A and B was modified with the complementary nucleic acids y and y′ that fuse units A and B together. The other three edges of the square-origami faces of the square-bipyramid units A and B were modified with the *trans*-azobenzene-functionalized toehold nucleic acids X and X′, respectively. Upon annealing of the nanostructure units A and B, a closed square-bipyramid nanostructure was formed that was stabilized by the cooperative hybridization of the duplexes y/y′ and the *trans*-azobenzene-stabilized duplex toeholds X/X′ on the other three base edges. Photoisomerization of the *trans*-azobenzene units to *cis*-azobenzene (UV irradiation) weakened the hybrids X/X′, resulting in their separation and the unlocking (opening) of the square-bipyramid structure. The bipyramid closed and open structures were imaged by AFM (Figure 22 B, panels I and II). Furthermore, by modifying the origami base with protruding nucleic acid Z′, Au nanoparticles modified with the nucleic acid Z were loaded on the *cis*-azobenzene open bipyramid structure by hybridization with the protruding tethers to form Z/Z′ duplex bridges (Figure 22 C). Subsequently, photoisomerization of the *cis*-azobenzene units to the *trans*-azobenzene state resulted in the closure of the system into the square-bipyramidal structure. Upon UV illumination of the Au NP-loaded square-bipyramid structure, the system opened due to the weakening of the three photoactive nucleic acid edges that yield *cis*-azobenzene functionalities. Treatment of the open bipyramid structure with the nucleic acid Z″ displaced the Z-functionalized Au NPs through the formation of the energetically stabilized Z′/Z″ duplex, resulting in the release of Z-functionalized Au NPs from the bipyramid structure. AFM measurements showed that the strand-displacement process and the release of the Au NPs from the open square-bipyramid structure is substantially more efficient than from the closed Au NPs-loaded nanostructure. Presumably, the photonic opening of the square-bipyramid exposes the NPs to the strand displacement process, resulting in their efficient release.

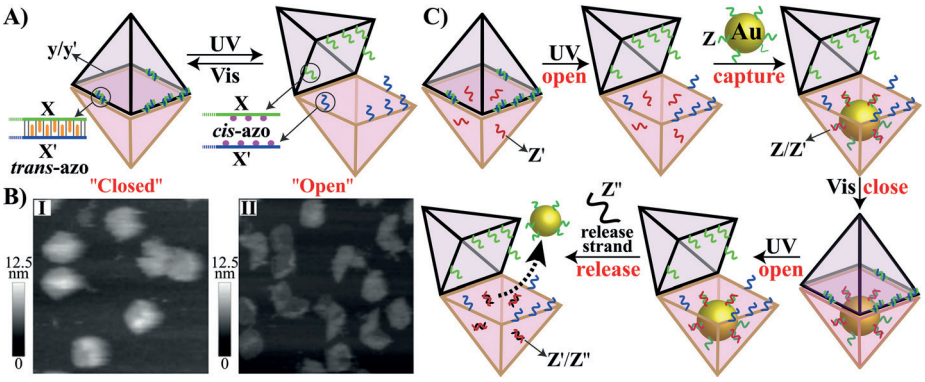

Figure 22. A) Synthesis of photoresponsive square-bipyramidal DNA origami nanocapsules, and the cyclic opening and closure of the bipyramidal structure by the cyclic photoisomerization of the *trans*-azobenzene units to the *cis*-azobenzene state and back. B) AFM images of the "closed" bipyramidal nanostructures (left) and of the photostimulated *cis*-azobenzene-functionalized "open" bipyramid nanostructures (right). C) Loading of the bipyramidal capsules with Au NPs and the photostimulated release of the Au NPs by photoisomerization of the *trans*-azobenzene units to the *cis*-azobenzene state, and the strand displacement of the in-capsule associated Au nanoparticles. Adapted with permission from Ref. [97]. Copyright 2014 Wiley-VCH.

4. Stimuli-Responsive Micelles and Vesicles as Functional Carriers

Lipid-modified oligonucleotides provide block copolymers that can assemble into micellar or vesicle structures in aqueous medium.[98] The hydrophobic core of micellar polymer–DNA structures may act as a reservoir for hydrophobic guest molecules, whereas the hydrophilic nucleic acid shell might provide cell-targeting or stimuli-responsive units for the release of the micellar loads. Similarly, DNA–lipid components can be integrated into the hydrophobic walls of vesicles.[99] The interior of the vesicles can act as a reservoir of hydrophilic loads and the DNA units incorporated in the vesicle walls may provide either cell-targeting units or functional units unlocking the walls. Different DNA–lipid block polymers were synthesized and the resulting micellar structures were characterized.[100,101] For example, the DNA-*b*-polypropylene oxide polymer **34**-*b*-PPO was synthesized[101] (Figure 23 A). The single-strand micelles exhibited a radius of (5.6 ± 0.5) nm, and hybridization of the hydrophilic nucleotide tethers with the complementary nucleic acid **35** had a minute effect on the size of the resulting micelles (5.3 ± 0.5) nm. In turn, treatment of the single-stranded micelles with a long DNA template $(\mathbf{35})_n$ consisting of constant repeat units complementary to the nucleotide tethers associated with the micelles resulted in rod-like micelles revealing a height of (1.95 ± 0.1) nm and length of (29.1 ± 6.5) nm (Figure 23 B). The internalization of the different polymeric particles into cells was examined, and it was found that the particles are nontoxic and that the rod-like particles penetrate more efficiently into cells than the spherical micelles.[102] The structures of DNA–lipid block copolymers can be controlled by the lengths of the hydrophilic nucleotide tethers, and the micelles could be enlarged by polymerization of the 3′-ends of the nucleotide tethers with the terminal deoxynucleotidyl transferase (TdT) in the presence of the dNTPs mixture and an appropriate primer.[103]

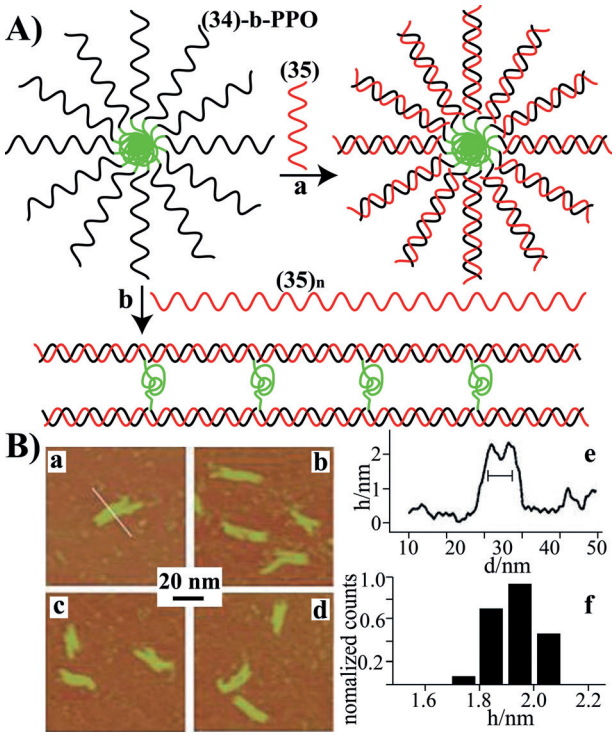

Figure 23. A) Self-assembly of **34**-*b*-PPO micelles, and the hybridization complementary nucleic acid **35** with the micelles. The hybridization of the **34**-functionalized PPO micelles with DNA chains composed of repeat units of **35** leads to rod-like micelles. B) AFM images of the resulting rod-like micelles (a–d), cross-section analysis of the rod-like micelles (e), and the height histogram of the micelles (f). Adapted with permission from Ref. [101]. Copyright 2007 Wiley-VCH.

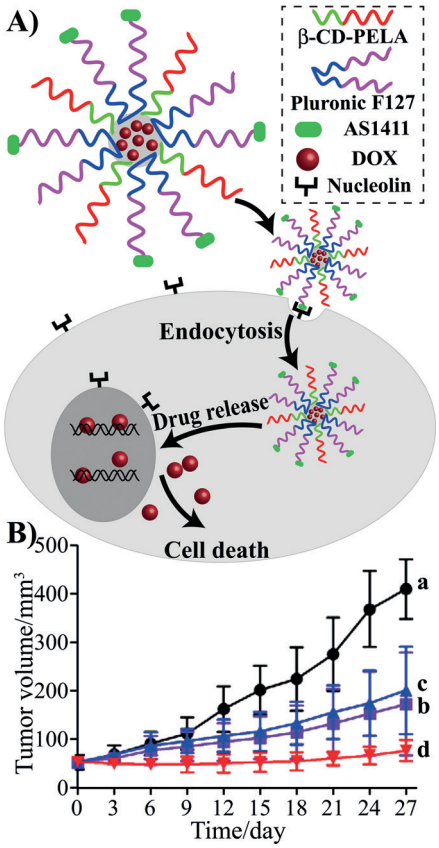

Figure 24. A) Incorporation of DOX-loaded pluronic acid F127/β-CD-PELA-AS1411 aptamer micelles into MCF-7 tumor-bearing mice, and the in vivo pH-stimulated release of DOX. B) Time-dependent tumor size changes upon intravenous injection into the tumor-infected mice with: a) Tumor without additive; b) tumor treated with free DOX; c) tumor treated with DOX-loaded aptamer-mutant-modified micelles; d) tumor treated with DOX-loaded aptamer-modified micelles. Adapted with permission from Ref. [104]. Copyright 2015, Elsevier.

The information encoded in the nucleic acid sequence comprising the DNA–polymer micelles was used to target the micelle carriers into cells, thus enabling the release of drug loads incorporated in the core of the micelles. For example, micelles composed of the AS1411-modified pluronic acid F127 and β-cyclodextrin-functionalized poly(ethylene glycol)-*b*-polylactide were prepared, and the anticancer drug DOX was incorporated into the hydrophobic core of the micelles.[104] The AS1411 aptamer guides the micelles to the nucleolin receptor sites associated with cancer cells resulting in nucleolin-mediated endocytosis of the micelles into the MCF-7 tumor cells and the intracellular release of DOX (Figure 24 A). The effect of the DOX-loaded aptamer-functionalized micelles on the growth of MCF-7 tumors in mice was examined (Figure 24 B). It was found that within 27 days the tumors treated with the DOX-loaded aptamer micelles revealed a tumor growth of ca. 50%, whereas untreated tumors grew by ca. 660%. Also, tumors treated with only DOX or with DOX-loaded random nucleic acid micelles grew by ca. 240% within this time interval. These results show the superior activity of the DOX-loaded AS1411-aptamer-functionalized micelles on the inhibition of the growth of the tumors, a phenomenon that was attributed to the effective nucleolin-mediated endocytosis of the drug-loaded micelles into the cancer cells resulting in the efficient targeted release of the drug.

Fluorophore-labeled DNA/polymer micelles were incorporated into cells and suggested as nanosensors for probing intracellular ingredients (e.g., ATP)[105] as well as functional labels for cell imaging.[106] Functional DNA/polymer micelles may also act as an active nanostructure for controlling cell proliferation, and thus provide a mechanism for the inhibition of the growth of cancer cells.[107] This is exemplified in Figure 25 A with the self-assembly of DNA–lipid units, consisting of a DNA hairpin **36** that is tethered to a hydrophobic chain of diacyllipid, into a micellar structure. The hairpin units included the recognition sequence for a segment of the *c-raf-1* mRNA of A549 lung cancer cells. These micelles were incorporated into the cell, resulting in the binding of the mRNA to the hairpin structure, a process that resulted in the suppression of cell growth. Figure 25 B depicts the cytotoxicity of the hairpin DNA/polymer micelles toward A549 cells, in comparison to the effect of a random DNA/polymer nanostructure on these cells. Evidently, the hairpin/DNA polymer micelles lead to an impressive cell death, due to the caging of the mRNA that prohibits gene expression.[107]

The design of DNA/polymer micelles of enhanced complexity enables the loading and release of the anticancer drug

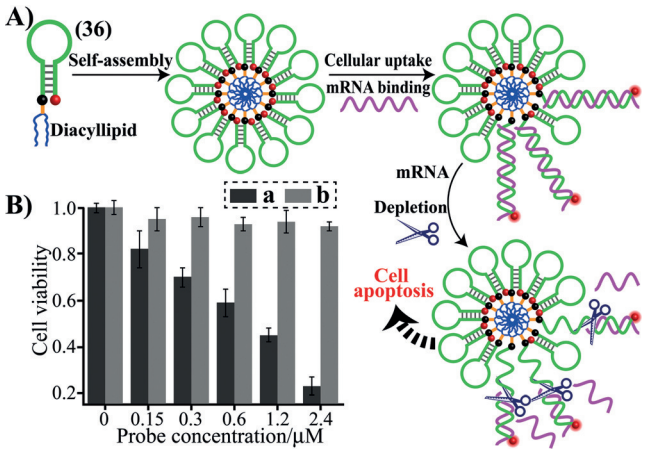

Figure 25. A) Synthesis of hairpin DNA-functionalized diacyllipid micelles and the intracellular degradation of the micelles by the mRNA opening of the hairpins, and the subsequent cleavage of the resulting duplex mRNA structures. B) Viability of A549 cells treated with different concentrations of the mRNA responsive hairpin DNA/lipid micelles (a, black) and control systems (b, gray). Adapted with permission from Ref. [107]. Copyright 2013 Wiley-VCH.

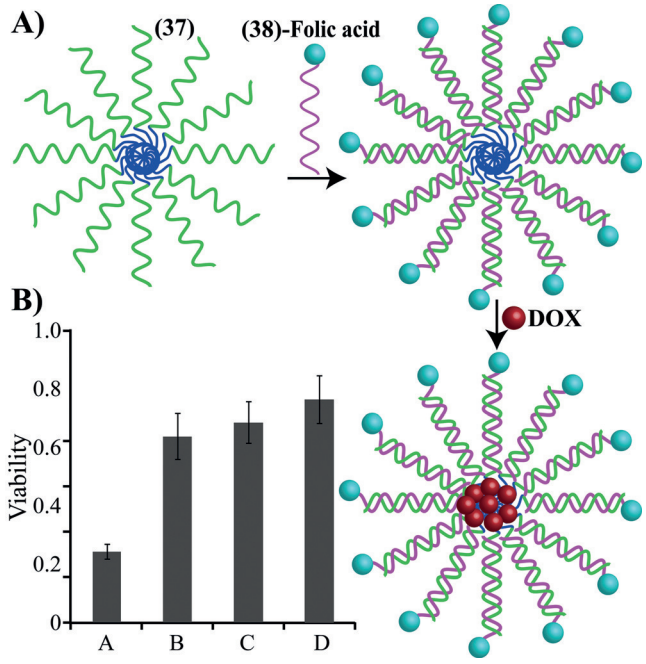

Figure 26. A) Synthesis of DOX-loaded DNA-*b*-PPO micelles functionalized with folic-acid-modified nucleic acids as cancer cell targeting units. B) Viability of human colon adenocarcinoma (Caco-2) cells upon treatment with: a) DOX-loaded micelles functionalized with targeting folic acid units; b) DOX-loaded micelles with free folic acid; c) DOX-loaded micelles; d) unloaded micelles functionalized with folic acid. Adapted with permission from Ref. [108]. Copyright 2008 Wiley-VCH.

by the micelles, and the targeting of the micelles to cancer cells. This is exemplified in Figure 26 A with the synthesis of the lipid–DNA polymers composed of the hydrophilic nucleic acid **37** tethered to poly(propylene oxide).[108] The hybridization of the folic-acid-modified nucleic acid **38** with the DNA tethers associated with the micelles generate the folic-acid-functionalized nanostructures that target the micelles to the folic acid receptors associated with cancer cells. The anticancer drug DOX was subsequently loaded into the core of the micelles (Figure 26 A). The drug-loaded folic-acid-modified micelles were then incorporated into human colon adenocarcinoma (Caco-2) cells and the effect of the hybrid micellar nanostructure on the viability of cancer cells was examined and compared to several control systems (Figure 26 B). Clearly, impressive cell death was observed with the DOX-loaded folic-acid-functionalized nanostructures, implying that the targeting and effective delivery of the drug into the cells has a pronounced effect on the cell viability.

Light-sensitive DNA block copolymer lipid vesicles have been synthesized and used as stimuli-responsive nanocarriers for the controlled release of loads.[109] The vesicles composed of 1,2-diphytanoyl-*sn*-glycero-3-phosphocholine were loaded with calcein and the lipid-DNA **39**-*b*-poly(propylene oxide) (DNA-*b*-PPO), was incorporated into the vesicles (Figure 27 A). The nucleic acid **40** functionalized with the photosensitizer BODIPY monoiodine was hybridized with the surface-DNA tethers, to yield photosensitizer-modified vesicles. Irradiation of the system at 530 nm under air resulted in singlet oxygen and reactive oxygen species that lead to the degradation of the vesicle walls and release of the calcein load

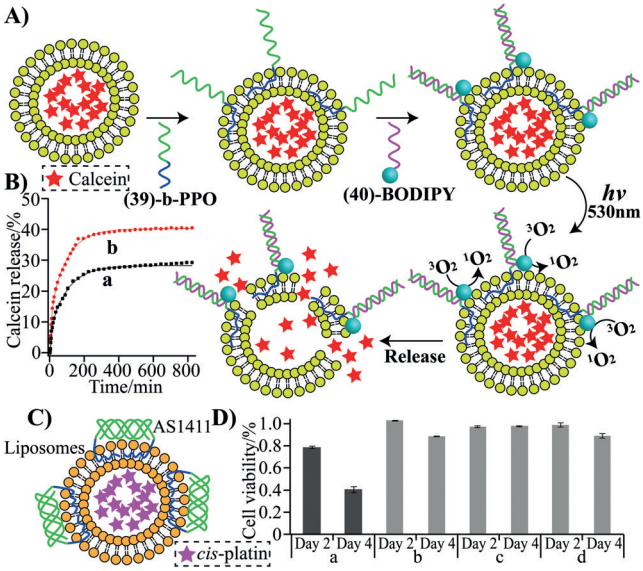

Figure 27. A) Synthesis of calcein-loaded lipid–DNA vesicles functionalized with the BODIPY photosensitizer. The photosensitizer-stimulated generation of reactive oxygen species degrades the vesicles and releases the loads. B) Time-dependent release of the calcein load upon irradiation of the vesicles for: a) 104 min; b) 164 min. Adapted with permission from Ref. [109]. Copyright 2013 Wiley-VCH. C) Structure of *cis*-platin-loaded AS1411-functionalized lipid–DNA liposomes. D) Viability of MCF-7 cells, and control systems, treated with: a) *cis*-platin-loaded AS1411-functionalized liposomes; b) Control system including *cis*-platin but lacking the AS1411 targeting aptamer; c) Unloaded AS1411-functionalized liposomes; d) Treatment of a non-cancerous cell with the *cis*-platin-loaded AS1411-functionalized liposomes. The cell viability of the different systems was monitored at day 2 and day 4 of treatment. Adapted with permission from Ref. [110]. Copyright 2009 Wiley-VCH.

(Figure 27B). As the irradiation time is prolonged, the release of the load is more effective. Similarly, liposomes composed of phosphatidylcholine, cholesterol, distearoyl phosphatidyl ethanolamine derivatized with methoxy poly(ethylene glycol), were loaded with the anticancer drug *cis*-platin.[110] The cholesterol-functionalized AS1411 aptamer was incorporated into the liposome wall, to yield an aptamer-modified drug-loaded liposome (Figure 27C). The aptamer units acted as targeting elements, which link the liposomes to cancer cells, and facilitate their penetration into the cell and the subsequent release of the drug. The *cis*-platin-loaded aptamer-functionalized liposomes were incorporated into MCF-7 cancer cells, and their effect on the cell viability was compared to several control systems, including liposomes lacking the cell-targeting aptamer units, or unloaded aptamer-modified liposomes (Figure 27D). Impressive cell death (ca. 60%) after four days exposure of the cancer cells to the drug-loaded aptamer-functionalized liposomes was observed, whereas a cell viability of ca. 100% was observed for the control systems.[110]

5. Summary and Outlook

Substantial recent research efforts are directed to implement nanomaterials for medical applications (nanomedicine).[111] The present Review discussed different DNA-functionalized nano-/microscale containers as stimuli-responsive systems for the controlled release of loads. Specifically, the use of MP SiO_2 NPs, the application of DNA-based microcapsules, and the use of nucleic-acid-functionalized micelles and vesicles as carriers has been addressed. The common dominator in all of these systems is the integration of DNA with the different carriers, yielding stimuli-responsive hybrids for the controlled release of loads. In this context, we highlighted that the encoded base sequences in the DNA units provide the instructive information to trigger, by external or environmental stimuli, the controlled release of loads from the different containments.

Stimuli-responsive DNA-modified MP SiO_2 NPs were extensively studied as carrying matrices for controlled release. Their nanometer dimensions, high surface area, high pore-loading capacities, low cytotoxicity, effective cell permeability, and ease to modify the nanoparticles by cell targeting antibodies, aptamers, or cell ligands, make SiO_2 NPs ideal drug carriers. Indeed, substantial progress was demonstrated, and many different stimuli-responsive DNA-capped MP SiO_2 NPs carriers were reported. The unlocking of the pores by external triggers and the release of the loads was demonstrated by different mechanisms. Also, the incorporation of anticancer-drug-loaded particles into cells, the triggered intracellular release of the drugs, and the effect of the released drugs on the viability of the cells were discussed. Important challenging issues in the application of MP SiO_2 NPs as drug carriers are still ahead of us: 1) The fundamental understanding of the mechanisms involved in the permeation of the NPs into cells is essential. Also, further methods to improve the selectivity of cell permeation (e.g., cancer cells vs. normal cells) and the targeting of the NPs into specific cells are required. 2) At present, most of the systems demonstrated the stimuli-controlled release of fluorescent anticancer drugs (e.g., DOX, CPT) or of fluorescent dyes as drug-release models. This is mainly due to the ease of quantitative monitoring the in vitro release rates of loads. The implementation of other analytical methods, e.g., HPLC, to probe the release of nonfluorescent drugs would broaden the spectrum of potential medical applications. 3) The systematic in vivo therapeutic examination of the stimuli-responsive DNA/MP SiO_2 NPs on living species such as mice, rats, and pigs is an important step toward the practical and economical application of these hybrid composites in future nanomedicine. 4) The immunogenicity of the different DNA-modified nanostructures is a further important subject to evaluate.

DNA-based microcapsules represent an interesting class of micro-/nanocontainers. Although substantial progress has been accomplished in the fabrication and cleavage of non-DNA capsules, limited advances were reported in the synthesis of functional DNA-based loaded micro-/nanocapsules, and their triggered opening to release loads. The use of nucleic acids as negatively charged polyelectrolytes was demonstrated and the enzymatic decomposition of these capsules by the hydrolytic cleavage of the biopolymers was reported. These studies did not, however, make use of the possibilities to encode information into the DNA coating of the microcapsules. Specifically, the introduction of recognition and catalytic functions into the DNA shells could provide new opportunities and challenges in the area of DNA nanotechnology. For example, all DNA shells composed of programmed aptamer cross-linked DNA layers, or metal-ion-dependent DNAzyme layers, may be envisaged. The triggered separation of the capsules by means of ligand–aptamer complexes or by the catalytic metal-ion-dependent DNAzyme-stimulated cleavage of the shells may be important paths to follow. Similarly, the ion-assisted cross-linking of the nucleic acid layers (e.g., by T-Hg^{2+}-T or C-Ag^{+}-C bridges) and the subsequent elimination of the shell-stabilizing ions by appropriate ligands (e.g., cystamine), could provide a general route to form and dissociate the capsules. Alternatively, the application of photoisomerizable intercalators, e.g., azobenzene units could allow the stabilization of cross-linked DNA shells and the subsequent dissociation by light. Furthermore, the stepwise assembly of the DNA shells could allow the programmed incorporation of aptameric tethers to the outer-shell layers, and these could target the capsules to specific cells. Also, the progress in designing two-dimensional[112] or three-dimensional[113] origami DNA nanostructures provides new means to assemble capsule-like nanostructures without the need to construct a layered polymer shell on a core particle template, followed by the dissolution of the core. By the appropriate design of protruding nucleic acid tethers on the origami scaffolds the incorporation of stimuli-responsive units on the nanostructures[114] and the programmed association of loads can be achieved. For example, a capsule-like stimuli-responsive DNA nanostructure acting as a robot system was realized.[115] Two clasps of origami units were modified with protruding nucleic acids and used as functional components to form a reservoir for binding molecular payloads and lock the reservoir by complementary base pairing.

By the appropriate design of the lock–DNA units, acting as specific aptamers against cellular biomarkers, the programmed unlocking of the DNA container and the release of payloads were demonstrated.

The use of stimuli-responsive micelles and vesicles as functional nanocarriers for the controlled release of loads is another interesting path to follow. Although the fundamental functions of these carriers have been demonstrated, important future issues need to be resolved. For example, the mechanisms associated with the incorporation of lipid–DNA micelles/vesicles into cells, the design of DNA-based micelles/vesicles of enhanced complexity, e.g., photoresponsive systems, and the in vivo application of these systems are challenging topics that need to be addressed.

The applications of the different stimuli-responsive containers discussed in the present Review have emphasized the use of the carriers for controlled drug release. Although the use of these functional DNA-hybrid systems is anticipated to have an impact on the developing area of nanomedicine; other applications for the programmed release of loads from the carriers may be envisaged. These include the programmed release of molecular or biomolecular loads from the carrier, which could provide innovative means for programmed synthesis, activation of enzyme cascades,[116] and the use of the systems for logic-gate operations.[117] Furthermore, other stimuli-responsive DNA-based materials such as hydrogels recently attract substantial research efforts.[118] The miniaturization of these materials in the form of nano-/micro-hydrogels is anticipated to introduce new dimensions to the field of drug release. We thus conclude that stimuli-responsive DNA-based hybrid nanomaterials have a bright future in nanomedicine.

Our research on stimuli-responsive nanoparticles and nanomaterials is supported by the NanoSensoMach ERC Advanced Grant No. 267574 under the EC FP7/2007-2013 program.

How to cite: *Angew. Chem. Int. Ed.* **2015**, *54*, 12212–12235
Angew. Chem. **2015**, *127*, 12380–12405

[1] F. Wang, C. H. Lu, I. Willner, *Chem. Rev.* **2014**, *114*, 2881–2941.

[2] a) K. Gehring, J. L. Leroy, M. Guéron, *Nature* **1993**, *363*, 561–565; b) J. L. Leroy, M. Gueron, J. L. Mergny, C. Helene, *Nucleic Acids Res.* **1994**, *22*, 1600–1606; c) S. Nonin, J. L. Leroy, *J. Mol. Biol.* **1996**, *261*, 399–414; d) D. Collin, K. Gehring, *J. Am. Chem. Soc.* **1998**, *120*, 4069–4072.

[3] a) D. Sen, W. Gilbert, *Nature* **1988**, *334*, 364–366; b) T. Simonsson, *Biol. Chem.* **2001**, *382*, 621–628; c) S. Burge, G. N. Parkinson, P. Hazel, A. K. Todd, S. Neidle, *Nucleic Acids Res.* **2006**, *34*, 5402–5415; d) J. T. Davis, G. P. Spada, *Chem. Soc. Rev.* **2007**, *36*, 296–313; e) G. W. Collie, G. N. Parkinson, *Chem. Soc. Rev.* **2011**, *40*, 5867–5892.

[4] a) V. Sklenar, J. Feigon, *Nature* **1990**, *345*, 836–838; b) R. Haner, P. B. Dervan, *Biochemistry* **1990**, *29*, 9761–9765; c) J. Völker, D. P. Botes, G. G. Lindsey, H. H. Klump, *J. Mol. Biol.* **1993**, *230*, 1278–1290; d) D. Leitner, W. Schroder, K. Weisz, *Biochemistry* **2000**, *39*, 5886–5892; e) A. Soto, J. Loo, L. Marky, *J. Am. Chem. Soc.* **2002**, *124*, 14355–14363; f) Y. Chen, S. H. Lee, C. Mao, *Angew. Chem. Int. Ed.* **2004**, *43*, 5335–5338; *Angew. Chem.* **2004**, *116*, 5449–5452.

[5] a) Y. Miyake, H. Togashi, M. Tashiro, H. Yamaguchi, S. Oda, M. Kudo, Y. Tanaka, Y. Kondo, R. Sawa, T. Fujimoto, T. Machinami, A. Ono, *J. Am. Chem. Soc.* **2006**, *128*, 2172–2173; b) Y. Tanaka, S. Oda, H. Yamaguchi, Y. Kondo, C. Kojima, A. Ono, *J. Am. Chem. Soc.* **2007**, *129*, 244–245; c) S. He, D. Li, C. Zhu, S. Song, L. Wang, Y. Long, C. Fan, *Chem. Commun.* **2008**, 4885–4887; d) C. W. Liu, Y. T. Hsieh, C. C. Huang, H. T. Chang, *Chem. Commun.* **2008**, 2242–2244; e) Z. Zhu, Y. Su, J. Li, D. Li, J. Zhang, S. Song, Y. Zhao, G. Li, C. Fan, *Anal. Chem.* **2009**, *81*, 7660–7666; f) T. Li, S. Dong, E. Wang, *Anal. Chem.* **2009**, *81*, 2144–2149.

[6] a) C. K. Chiang, C. C. Huang, C. W. Liu, H. T. Chang, *Anal. Chem.* **2008**, *80*, 3716–3721; b) A. Ono, S. Q. Cao, H. Togashi, M. Tashiro, T. Fujimoto, T. Machinami, S. Oda, Y. Miyake, I. Okamoto, Y. Tanaka, *Chem. Commun.* **2008**, 4825–4827; c) R. Freeman, T. Finder, I. Willner, *Angew. Chem. Int. Ed.* **2009**, *48*, 7818–7821; *Angew. Chem.* **2009**, *121*, 7958–7961; d) Y. Wen, F. Xing, S. He, S. Song, L. Wang, Y. Long, D. Li, C. Fan, *Chem. Commun.* **2010**, *46*, 2596–2598; e) K. S. Park, C. Jung, H. G. Park, *Angew. Chem. Int. Ed.* **2010**, *49*, 9757–9760; *Angew. Chem.* **2010**, *122*, 9951–9954.

[7] a) J. SantaLucia, D. Hicks, *Annu. Rev. Biophys. Biomol. Struct.* **2004**, *33*, 415–440; b) D. Y. Zhang, A. J. Turberfield, B. Yurke, E. Winfree, *Science* **2007**, *318*, 1121–1125; c) D. Y. Zhang, E. Winfree, *J. Am. Chem. Soc.* **2009**, *131*, 17303–17314; d) D. Soloveichik, G. Seelig, E. Winfree, *Proc. Natl. Acad. Sci. USA* **2010**, *107*, 5393–5398; e) D. Y. Zhang, G. Seelig, *Nat. Chem.* **2011**, *3*, 103–113.

[8] a) S. Tyagi, F. Kramer, *Nat. Biotechnol.* **1996**, *14*, 303–308; b) J. Li, X. Fang, S. Schuster, W. Tan, *Angew. Chem. Int. Ed.* **2000**, *39*, 1049–1052; *Angew. Chem.* **2000**, *112*, 1091–1094; c) P. Zhang, T. Beck, W. Tan, *Angew. Chem. Int. Ed.* **2001**, *40*, 402–405; *Angew. Chem.* **2001**, *113*, 416–419; d) K. Fujimoto, H. Shimizu, M. Inouye, *J. Org. Chem.* **2004**, *69*, 3271–3275; e) I. Nesterova, S. Erdem, S. Pakhomov, R. Hammer, S. Soper, *J. Am. Chem. Soc.* **2009**, *131*, 2432–2433; f) S. Song, Z. Liang, J. Zhang, L. Wang, G. Li, C. Fan, *Angew. Chem. Int. Ed.* **2009**, *48*, 8670–8674; *Angew. Chem.* **2009**, *121*, 8826–8830; g) R. Häner, S. Biner, S. Langenegger, T. Meng, V. Malinovskii, *Angew. Chem. Int. Ed.* **2010**, *49*, 1227–1230; *Angew. Chem.* **2010**, *122*, 1249–1252; h) A. Jayagopal, K. Halfpenny, J. Perez, D. Wright, *J. Am. Chem. Soc.* **2010**, *132*, 9789–9796.

[9] a) D. Liu, S. Balasubramanian, *Angew. Chem. Int. Ed.* **2003**, *42*, 5734–5736; *Angew. Chem.* **2003**, *115*, 5912–5914; b) S. Modi, M. G. Swetha, D. Goswami, G. D. Gupta, S. Mayor, Y. Krishnan, *Nat. Nanotechnol.* **2009**, *4*, 325–330; c) A. Idili, A. Vallée-Bélisle, F. Ricci, *J. Am. Chem. Soc.* **2014**, *136*, 5836–9583; d) T. Li, M. Famulok, *J. Am. Chem. Soc.* **2013**, *135*, 1593–1599.

[10] a) S. Shimron, J. Elbaz, A. Henning, I. Willner, *Chem. Commun.* **2010**, *46*, 3250–3252; b) C. H. Lu, X. J. Qi, R. Orbach, H. H. Yang, I. Mironi-Harpaz, D. Seliktar, I. Willner, *Nano Lett.* **2013**, *13*, 1298–1302; c) W. Guo, X. J. Qi, R. Orbach, C. H. Lu, L. Freage, I. Mironi-Harpaz, D. Seliktar, H. H. Yang, I. Willner, *Chem. Commun.* **2014**, *50*, 4065–4068.

[11] a) H. Asanuma, T. Takarada, T. Yoshida, D. Tamaru, X. Liang, M. Komiyama, *Angew. Chem. Int. Ed.* **2001**, *40*, 2671–2673; *Angew. Chem.* **2001**, *113*, 2743–2745; b) H. Kashida, T. Fujii, H. Asanuma, *Org. Biomol. Chem.* **2008**, *6*, 2892–2899; c) X. Liang, T. Mochizuki, H. Asanuma, *Small* **2009**, *5*, 1761–1768.

[12] a) J. F. Lee, G. M. Stovall, A. D. Ellington, *Curr. Opin. Struct. Biol.* **2006**, *10*, 282–289; b) I. Willner, M. Zayats, *Angew. Chem. Int. Ed.* **2007**, *46*, 6408–6418; *Angew. Chem.* **2007**, *119*, 6528–6538; c) A. A. Goulko, F. Li, X. C. Le, *TrAC Trends Anal. Chem.* **2009**, *28*, 878–892; d) M. Famulok, G. Mayer, *Acc. Chem. Res.* **2011**, *44*, 1349–1358.

[13] a) C. Tuerk, L. Gold, *Science* **1990**, *249*, 505 – 510; b) A. D. Ellington, J. W. Szostak, *Nature* **1990**, *346*, 818 – 822; c) S. E. Osborne, A. D. Ellington, *Chem. Rev.* **1997**, *97*, 349 – 370.

[14] a) R. R. Breaker, G. F. Joyce, *Chem. Biol.* **1994**, *1*, 223 – 229; b) G. F. Joyce, *Annu. Rev. Biochem.* **2004**, *73*, 791 – 836; c) M. Famulok, J. S. Hartig, G. Mayer, *Chem. Rev.* **2007**, *107*, 3715 – 3743; d) G. F. Joyce, *Angew. Chem. Int. Ed.* **2007**, *46*, 6420 – 6436; *Angew. Chem.* **2007**, *119*, 6540 – 6557; e) I. Willner, B. Shlyahovsky, M. Zayats, B. Willner, *Chem. Soc. Rev.* **2008**, *37*, 1153 – 1165.

[15] a) P. Travascio, Y. Li, D. Sen, *Chem. Biol.* **1998**, *5*, 505 – 517; b) P. Travascio, A. J. Bennet, D. Y. Wang, D. Sen, *Chem. Biol.* **1999**, *6*, 779 – 787; c) P. Travascio, P. K. Witting, A. G. Mauk, D. Sen, *J. Am. Chem. Soc.* **2001**, *123*, 1337 – 1348.

[16] a) R. K. Saiki, D. H. Gelfand, S. Stoffel, S. J. Scharf, R. Higuchi, G. T. Horn, K. B. Mullis, H. A. Erlich, *Science* **1988**, *239*, 487 – 491; b) A. R. Pavlov, N. V. Pavlova, S. A. Kozyavkin, A. I. Slesarev, *Trends Biotechnol.* **2004**, *22*, 253 – 260; c) Q. Guo, X. Yang, K. Wang, W. Tan, W. Li, H. Tang, H. Li, *Nucleic Acids Res.* **2009**, *37*, e20.

[17] a) P. Widlak, W. T. Garrard, *J. Cell. Biochem.* **2005**, *94*, 1078 – 1087; b) B. L. Stoddard, *Q. Rev. Biophys.* **2005**, *38*, 49 – 95; c) K. Calvin, H. Li, *Cell. Mol. Life Sci.* **2008**, *65*, 1176 – 1185.

[18] a) Y. Weizmann, M. K. Beissenhirtz, Z. Cheglakov, R. Nowarski, M. Kotler, I. Willner, *Angew. Chem. Int. Ed.* **2006**, *45*, 7384 – 7388; *Angew. Chem.* **2006**, *118*, 7544 – 7548; b) B. Shlyahovsky, D. Li, Y. Weizmann, R. Nowarski, M. Kotler, I. Willner, *J. Am. Chem. Soc.* **2007**, *129*, 3814 – 3815; c) D. Li, A. Wieckowska, I. Willner, *Angew. Chem. Int. Ed.* **2008**, *47*, 3927 – 3931; *Angew. Chem.* **2008**, *120*, 3991 – 3995.

[19] a) D. Mukherjee, D. T. Fritz, W. J. Kilpatrick, M. Gao, J. Wilusz, *Methods Mol. Biol.* **2004**, *257*, 193 – 212; b) S. West, N. Gromak, N. J. Proudfoot, *Nature* **2004**, *432*, 522 – 525.

[20] F. Wang, X. Liu, I. Willner, *Angew. Chem. Int. Ed.* **2015**, *54*, 1098 – 1129; *Angew. Chem.* **2015**, *127*, 1112 – 1144.

[21] a) H. Yan, X. Zhang, Z. Shen, N. C. Seeman, *Nature* **2002**, *415*, 62 – 65; b) N. C. Seeman, *Trends Biochem. Sci.* **2005**, *30*, 119 – 125; c) F. Wang, B. Willner, I. Willner, *Top. Curr. Chem.* **2014**, *354*, 279 – 338; d) M. K. Beissenhirtz, I. Willner, *Org. Biomol. Chem.* **2006**, *4*, 3392 – 3401; e) J. Bath, A. J. Turberfield, *Nat. Nanotechnol.* **2007**, *2*, 275 – 284; f) C. Teller, I. Willner, *Curr. Opin. Biotechnol.* **2010**, *21*, 376 – 391; g) Y. Krishnan, F. C. Simmel, *Angew. Chem. Int. Ed.* **2011**, *50*, 3124 – 3156; *Angew. Chem.* **2011**, *123*, 3180 – 3215.

[22] a) I. Willner, B. Willner, *Nano Lett.* **2010**, *10*, 3805 – 3815; b) F. Li, Y. Huang, Q. Yang, Z. Zhong, D. Li, L. Wang, S. Song, C. Fan, *Nanoscale* **2010**, *2*, 1021 – 1026; c) C. H. Lu, J. Li, J. J. Liu, H. H. Yang, X. Chen, G. N. Chen, *Chem. Eur. J.* **2010**, *16*, 4889 – 4894; d) Y. V. Gerasimova, D. M. Kolpashchikov, *Chem. Biol.* **2010**, *17*, 104 – 106; e) F. Wang, J. Elbaz, R. Orbach, N. Magen, I. Willner, *J. Am. Chem. Soc.* **2011**, *133*, 17149 – 17151; f) S. Shimron, F. Wang, R. Orbach, I. Willner, *Anal. Chem.* **2012**, *84*, 1042 – 1048; g) Y. Du, B. Li, E. Wang, *Acc. Chem. Res.* **2013**, *46*, 203 – 213.

[23] a) D. M. Kolpashchikov, *J. Am. Chem. Soc.* **2008**, *130*, 2934 – 2935; b) T. Li, L. Shi, E. Wang, S. Dong, *Chem. Eur. J.* **2009**, *15*, 1036 – 1042; c) J. Liu, Z. Cao, Y. Lu, *Chem. Rev.* **2009**, *109*, 1948 – 1998; d) F. Wang, J. Elbaz, C. Teller, I. Willner, *Angew. Chem. Int. Ed.* **2011**, *50*, 295 – 299; *Angew. Chem.* **2011**, *123*, 309 – 313; e) G. Pelossof, R. Tel-Vered, I. Willner, *Anal. Chem.* **2012**, *84*, 3703 – 3709; f) F. Wang, C. H. Lu, X. Liu, L. Freage, I. Willner, *Anal. Chem.* **2014**, *86*, 1614 – 1621.

[24] a) M. N. Stojanović, D. Stefanović, *J. Am. Chem. Soc.* **2003**, *125*, 6673 – 6676; b) M. N. Stojanovic, S. Semova, D. Kolpashchikov, J. Macdonald, C. Morgan, D. Stefanovic, *J. Am. Chem. Soc.* **2005**, *127*, 6914 – 6915; c) G. Seelig, D. Soloveichik, D. Y. Zhang, E. Winfree, *Science* **2006**, *314*, 1585 – 1588; d) J. Macdonald, Y. Li, M. Sutovic, H. Lederman, K. Pendri, W. Lu, B. L. Andrews, D. Stefanovic, M. N. Stojanovic, *Nano Lett.* **2006**, *6*, 2598 – 2603; e) J. Elbaz, O. Lioubashevski, F. Wang, F. Remacle, R. D. Levine, I. Willner, *Nat. Nanotechnol.* **2010**, *5*, 417 – 422; f) L. Qian, E. Winfree, *Science* **2011**, *332*, 1196 – 1201; g) J. Elbaz, F. Wang, F. Remacle, I. Willner, *Nano Lett.* **2012**, *12*, 6049 – 6054; h) R. Orbach, L. Mostinski, F. Wang, I. Willner, *Chem. Eur. J.* **2012**, *18*, 14689 – 14694.

[25] a) A. Saghatelian, N. H. Völcker, K. M. Guckian, V. S. Lin, M. R. Ghadiri, *J. Am. Chem. Soc.* **2003**, *125*, 346 – 347; b) B. Shlyahovsky, Y. Li, O. Lioubashevski, J. Elbaz, I. Willner, *ACS Nano* **2009**, *3*, 1831 – 1843; c) T. Li, E. Wang, S. Dong, *J. Am. Chem. Soc.* **2009**, *131*, 15082 – 15083; d) R. Pei, E. Matamoros, M. Liu, D. Stefanovic, M. N. Stojanovic, *Nat. Nanotechnol.* **2010**, *5*, 773 – 777; e) T. Li, L. Zhang, J. Ai, S. Dong, E. Wang, *ACS Nano* **2011**, *5*, 6334 – 6338; f) H. Pei, L. Liang, G. Yao, J. Li, Q. Huang, C. Fan, *Angew. Chem. Int. Ed.* **2012**, *51*, 9020 – 9024; *Angew. Chem.* **2012**, *124*, 9154 – 9158; g) R. Orbach, F. Wang, O. Lioubashevski, R. D. Levine, F. Remacle, I. Willner, *Chem. Sci.* **2014**, *5*, 3381 – 3387; h) R. Orbach, S. Lilienthal, M. Klein, R. D. Levine, F. Remacle, I. Willner, *Chem. Sci.* **2015**, *6*, 1288 – 1292.

[26] a) L. Chen, R. K. Singh, P. Webley, *Microporous Mesoporous Mater.* **2007**, *102*, 159 – 170; b) Y. L. Cao, J. M. Cao, M. B. Zheng, J. S. Liu, G. B. Ji, *J. Solid State Chem.* **2007**, *180*, 792 – 798; c) Y. Chen, E. Stathatos, D. D. Dionysiou, *Surf. Coat. Technol.* **2008**, *202*, 1944 – 1950; d) J. Górka, M. Jaroniec, *Carbon* **2011**, *49*, 154 – 160.

[27] a) C. T. Kresge, M. E. Leonowicz, W. J. Roth, J. C. Vartuli, J. S. Beck, *Nature* **1992**, *359*, 710 – 712; b) N. Negishi, T. Iyoda, K. Hashimoto, A. Fujishima, *Chem. Lett.* **1995**, *24*, 841 – 842; c) M. Grün, I. Lauer, K. K. Unge, *Adv. Mater.* **1997**, *9*, 254 – 257; d) D. Brühwiler, *Nanoscale* **2010**, *2*, 887 – 892; e) J. Zhao, P. Wan, J. Xiang, T. Tong, L. Dong, Z. Gao, X. Shen, H. Tong, *Microporous Mesoporous Mater.* **2011**, *138*, 200 – 206; f) M. Colilla, B. Gonzalez, M. Vallet-Regi, *Biomater. Sci.* **2013**, *1*, 114 – 134.

[28] a) S. Tao, G. Li, *Colloid Polym. Sci.* **2007**, *285*, 721 – 728; b) T. Wagner, S. Haffer, C. Weinberger, D. Klaus, M. Tiemann, *Chem. Soc. Rev.* **2013**, *42*, 4036 – 4053.

[29] a) M. Vallet-Regí, F. Balas, D. Arcos, *Angew. Chem. Int. Ed.* **2007**, *46*, 7548 – 7558; *Angew. Chem.* **2007**, *119*, 7692 – 7703; b) M. Liong, J. Lu, M. Kovochich, T. Xia, S. G. Ruehm, A. E. Nel, F. Tamanoi, J. I. Zink, *ACS Nano* **2008**, *2*, 889 – 896; c) Y. Zhao, B. G. Trewyn, I. I. Slowing, V. S.-Y. Lin, *J. Am. Chem. Soc.* **2009**, *131*, 3462 – 3463.

[30] a) Y. Sakamoto, M. Kaneda, O. Terasaki, D. Y. Zhao, J. M. Kim, G. Stuckyk, H. J. Shin, R. Ryoo, *Nature* **2000**, *408*, 449 – 453; b) J. Kim, H. S. Kim, N. Lee, T. Kim, H. Kim, T. Yu, I. C. Song, W. K. Moon, T. Hyeon, *Angew. Chem. Int. Ed.* **2008**, *47*, 8438 – 8441; *Angew. Chem.* **2008**, *120*, 8566 – 8569; c) C.-P. Tsai, Y. Hung, Y.-H. Chou, D.-M. Huang, J.-K. Hsiao, C. Chang, Y.-C. Chen, C.-Y. Mou, *Small* **2008**, *4*, 186 – 191.

[31] a) S. Xiang, Y. Zhang, Q. Xin, C. Li, *Chem. Commun.* **2002**, 2696 – 2697; b) S. Huh, H.-T. Chen, J. W. Wiench, M. Pruski, V. S.-Y. Lin, *Angew. Chem. Int. Ed.* **2005**, *44*, 1826 – 1830; *Angew. Chem.* **2005**, *117*, 1860 – 1864; c) F. Jiao, H. Frei, *Angew. Chem. Int. Ed.* **2009**, *48*, 1841 – 1844; *Angew. Chem.* **2009**, *121*, 1873 – 1876.

[32] a) Q. Yang, S. Wang, P. Fan, L. Wang, Y. Di, K. Lin, F.-S. Xiao, *Chem. Mater.* **2005**, *17*, 5999 – 6003; b) Q. Gao, Y. Xu, D. Wu, W. Shen, F. Deng, *Langmuir* **2010**, *26*, 17133 – 17138; c) H. Zheng, Y. Wang, S. Che, *J. Phys. Chem. C* **2011**, *115*, 16803 – 16813.

[33] C.-Y. Lai, B. G. Trewyn, D. M. Jeftinija, K. Jeftinija, S. Xu, S. Jeftinija, V. S.-Y. Lin, *J. Am. Chem. Soc.* **2003**, *125*, 4451 – 4459.

[34] a) R. Liu, X. Zhao, T. Wu, P. Feng, *J. Am. Chem. Soc.* **2008**, *130*, 14418 – 14419; b) Z. Luo, K. Cai, Y. Hu, L. Zhao, P. Liu, L. Duan, W. Yang, *Angew. Chem. Int. Ed.* **2011**, *50*, 640 – 643; *Angew. Chem.* **2011**, *123*, 666 – 669.

[35] a) X. Wan, D. Wang, S. Liu, *Langmuir* **2010**, *26*, 15574 – 15579; b) Z. Zhang, D. Balogh, F. Wang, R. Tel-Vered, N. Levy, S. Y. Sung, R. Nechushtai, I. Willner, *J. Mater. Chem. B* **2013**, *1*, 3159 – 3166.

[36] E. Aznar, R. Casasus, B. Garcia-Acosta, M. D. Marcos, R. Martinez-Manez, F. Sancenon, J. Soto, P. Amoros, *Adv. Mater.* **2007**, *19*, 2228 – 2231.

[37] K. Zhang, W. Wu, K. Guo, J. Chen, P. Zhang, *Langmuir* **2010**, *26*, 7971 – 7980.

[38] a) C. R. Thomas, D. P. Ferris, J.-H. Lee, E. Choi, M. H. Cho, E. S. Kim, J. F. Stoddart, J.-S. Shin, J. Cheon, J. I. Zink, *J. Am. Chem. Soc.* **2010**, *132*, 10623 – 10625; b) P. J. Chen, S. H. Hu, C. S. Hsiao, Y. Y. Chen, D. M. Liu, S. Y. Chen, *J. Mater. Chem.* **2011**, *21*, 2535 – 2543; c) E. Bringas, O. Koysuren, D. V. Quach, M. Mahmoudi, E. Aznar, J. D. Roehling, M. D. Marcos, R. Martinez-Manez, P. Stroeve, *Chem. Commun.* **2012**, *48*, 5647 – 5649.

[39] a) H. Takahashi, B. Li, T. Sasaki, C. Miyazaki, T. Kajino, S. Inagaki, *Chem. Mater.* **2000**, *12*, 3301 – 3305; b) C. Lei, Y. Shin, J. Liu, E. J. Ackerman, *J. Am. Chem. Soc.* **2002**, *124*, 11242 – 11243; c) S. Giri, B. G. Trewyn, M. P. Stellmaker, V. S.-Y. Lin, *Angew. Chem. Int. Ed.* **2005**, *44*, 5038 – 5044; *Angew. Chem.* **2005**, *117*, 5166 – 5172; d) C. Park, H. Kim, S. Kim, C. Kim, *J. Am. Chem. Soc.* **2009**, *131*, 16614 – 16615.

[40] Y. Zhao, B. G. Trewyn, I. I. Slowing, V. S.-Y. Lin, *J. Am. Chem. Soc.* **2009**, *131*, 8398 – 8400.

[41] a) B. Hildebrandt, P. Wust, O. Ahlers, A. Dieing, G. Sreenivasa, T. Kerner, R. Felix, H. Riess, *Crit. Rev. Oncol. Hematol.* **2002**, *43*, 33 – 56; b) J. Croissant, J. I. Zink, *J. Am. Chem. Soc.* **2012**, *134*, 7628 – 7631.

[42] a) A. Popat, S. B. Hartono, F. Stahr, J. Liu, S. Z. Qiao, G. Q. Lu, *Nanoscale* **2011**, *3*, 2801 – 2818; b) P. Nadrah, O. Planinsek, M. Gaberscek, *J. Mater. Sci.* **2014**, *49*, 481 – 495.

[43] a) Y. Xing, E. Cheng, Y. Yang, P. Chen, T. Zhang, Y. Sun, Z. Yang, D. Liu, *Adv. Mater.* **2011**, *23*, 1117 – 1121; b) M. S. Hung, O. Kurosawa, M. Washizu, *Mol. Cell. Probes* **2012**, *26*, 107 – 112.

[44] C. Chen, J. Geng, F. Pu, X. Yang, J. Ren, X. Qu, *Angew. Chem. Int. Ed.* **2011**, *50*, 882 – 886; *Angew. Chem.* **2011**, *123*, 912 – 916.

[45] Z. Zhang, D. Balogh, F. Wang, S. Y. Sung, R. Nechushtai, I. Willner, *ACS Nano* **2013**, *7*, 8455 – 8468.

[46] C. Temme, R. Weissbach, H. Lilie, C. Wilson, A. Meinhart, S. Meyer, R. Golbik, A. Schierhorn, E. Wahle, *J. Biol. Chem.* **2009**, *284*, 8337 – 8348.

[47] R. J. Devenish, M. Prescott, G. M. Boyle, P. Nagley, *J. Bioenerg. Biomembr.* **2000**, *32*, 507 – 515.

[48] S. Zhou, X. Du, F. Cui, X. Zhang, *Small* **2014**, *10*, 980 – 988.

[49] E. Climent, R. Martínez-Máñez, F. Sancenón, M. D. Marcos, J. Soto, A. Maquieira, P. Amorós, *Angew. Chem. Int. Ed.* **2010**, *49*, 7281 – 7283; *Angew. Chem.* **2010**, *122*, 7439 – 7441.

[50] W. P. Li, P. Y. Liao, C. H. Su, C. S. Yeh, *J. Am. Chem. Soc.* **2014**, *136*, 10062 – 10075.

[51] C. Chen, F. Pu, Z. Huang, Z. Liu, J. Ren, X. Qu, *Nucleic Acids Res.* **2011**, *39*, 1638 – 1644.

[52] L. Chen, J. Di, C. Cao, Y. Zhao, Y. Ma, J. Luo, Y. Wen, W. Song, Y. Song, L. Jiang, *Chem. Commun.* **2011**, *47*, 2850 – 2852.

[53] Z. Zhang, F. Wang, Y. S. Sohn, R. Nechushtai, I. Willner, *Adv. Funct. Mater.* **2014**, *24*, 5662 – 5670.

[54] M. Chen, S. Yang, X. He, K. Wang, P. Qiu, D. He, *J. Mater. Chem. B* **2014**, *2*, 6064 – 6071.

[55] X. He, Y. Zhao, D. He, K. Wang, F. Xu, J. Tang, *Langmuir* **2012**, *28*, 12909 – 12915.

[56] a) L. Chen, Y. Wen, B. Su, J. Di, Y. Song, L. Jiang, *J. Mater. Chem.* **2011**, *21*, 13811 – 13816; b) C. L. Zhu, C. H. Lu, X. Y. Song, H. H. Yang, X. R. Wang, *J. Am. Chem. Soc.* **2011**, *133*, 1278 – 1281.

[57] P. Zhang, F. Cheng, R. Zhou, J. Cao, J. Li, C. Burda, Q. Min, J. J. Zhu, *Angew. Chem. Int. Ed.* **2014**, *53*, 2371 – 2375; *Angew. Chem.* **2014**, *126*, 2403 – 2407.

[58] Z. Li, Z. Liu, M. Yin, X. Yang, Q. Yuan, J. Ren, X. Qu, *Biomacromolecules* **2012**, *13*, 4257 – 4263.

[59] Z. Zhang, D. Balogh, F. Wang, I. Willner, *J. Am. Chem. Soc.* **2013**, *135*, 1934 – 1940.

[60] Z. Zhang, F. Wang, D. Balogh, I. Willner, *J. Mater. Chem. B* **2014**, *2*, 4449 – 4455.

[61] a) F. Pu, Z. Liu, X. Yang, J. Ren, X. Qu, *Chem. Commun.* **2011**, *47*, 6024 – 6026; b) F. Pu, Z. Liu, J. Ren, X. Qu, *Chem. Commun.* **2013**, *49*, 2305 – 2307; c) F. Pu, J. Ren, X. Qu, *Adv. Mater.* **2014**, *26*, 5742 – 5757.

[62] a) M. Diez, M. Arroyo, F. J. Cerdan, M. Munoz, M. A. Martin, J. L. Balibrea, *Oncology* **1989**, *46*, 230 – 234; b) S. K. Gupta, V. K. Shukla, M. P. Vaidya, S. K. Roy, S. Gupta, *J. Surg. Oncol.* **1993**, *52*, 172 – 175.

[63] a) J. L. Wike-Hooley, J. Haveman, H. S. Reinhold, *Radiother. Oncol.* **1984**, *2*, 343 – 366; b) P. Vaupel, F. Kallinowski, P. Okunieff, *Cancer Res.* **1989**, *49*, 6449 – 6465.

[64] Q. Yuan, Y. Zhang, T. Chen, D. Lu, Z. Zhao, X. Zhang, Z. Li, C.-H. Yan, W. Tan, *ACS Nano* **2012**, *6*, 6337 – 6344.

[65] Y. Wen, L. Xu, W. Wang, D. Wang, H. Du, X. Zhang, *Nanoscale* **2012**, *4*, 4473 – 4476.

[66] D. He, X. He, K. Wang, J. Cao, Y. Zhao, *Adv. Funct. Mater.* **2012**, *22*, 4704 – 4710.

[67] C. Chen, L. Zhou, J. Geng, J. Ren, X. Qu, *Small* **2013**, *9*, 2793 – 2800.

[68] X. Yang, X. Liu, Z. Liu, F. Pu, J. Ren, X. Qu, *Adv. Mater.* **2012**, *24*, 2890 – 2895.

[69] N. Li, Z. Yu, W. Pan, Y. Han, T. Zhang, B. Tang, *Adv. Funct. Mater.* **2013**, *23*, 2255 – 2262.

[70] a) Y. Wang, A. S. Angelatos, F. Caruso, *Chem. Mater.* **2008**, *20*, 848 – 858; b) L. L. del Mercato, P. Rivera-Gil, A. Z. Abbasi, M. Ochs, C. Ganas, I. Zins, C. Sönnichsen, W. J. Parak, *Nanoscale* **2010**, *2*, 458 – 467; c) A. G. Skirtach, A. M. Yashchenok, H. Möhwald, *Chem. Commun.* **2011**, *47*, 12736 – 12746; d) W. Tong, X. Song, C. Gao, *Chem. Soc. Rev.* **2012**, *41*, 6103 – 6124.

[71] a) Y. J. Wang, V. Bansal, A. N. Zelikin, F. Caruso, *Nano Lett.* **2008**, *8*, 1741 – 1745; b) B. G. De Geest, S. De Koker, G. B. Sukhorukov, O. Kreft, W. J. Parak, A. G. Skirtach, J. Demeester, S. C. De Smedt, W. E. Hennink, *Soft Matter* **2009**, *5*, 282 – 291; c) L. J. De Cock, S. De Koker, B. G. De Geest, J. Grooten, C. Vervaet, J. P. Remon, G. B. Sukhorukov, M. N. Antipina, *Angew. Chem. Int. Ed.* **2010**, *49*, 6954 – 6973; *Angew. Chem.* **2010**, *122*, 7108 – 7127; d) S. De Koker, B. N. Lambrecht, M. A. Willart, Y. van Kooyk, J. Grooten, C. Vervaet, J. P. Remon, B. G. De Geest, *Chem. Soc. Rev.* **2011**, *40*, 320 – 339; e) M. M. de Villiers, Y. M. Lvov, *Adv. Drug Delivery Rev.* **2011**, *63*, 699 – 700.

[72] H. Ai, *Adv. Drug Delivery Rev.* **2011**, *63*, 772 – 788.

[73] a) L. J. Ignarro, G. M. Buga, K. S. Wood, R. E. Byrns, G. Chaudhuri, *Proc. Natl. Acad. Sci. USA* **1987**, *84*, 9265 – 9269; b) T. A. Duchesne, J. Q. Brown, K. B. Guice, Y. M. Lvov, M. J. McShane, *Sens. Mater.* **2002**, *14*, 293 – 308; c) R. Srivastava, M. J. McShane, *J. Microencapsulation* **2005**, *22*, 397 – 411; d) O. Kreft, A. M. Javier, G. B. Sukhorukov, W. J. Parak, *J. Mater. Chem.* **2007**, *17*, 4471 – 4476; e) S. Amemori, M. Matsusaki, M. Akashi, *Chem. Lett.* **2010**, *39*, 42 – 43.

[74] W. Qi, X. H. Yan, J. B. Fei, A. H. Wang, Y. Cui, J. B. Li, *Biomaterials* **2009**, *30*, 2799 – 2806.

[75] A. G. Skirtach, B. G. De Geest, A. Mamedov, A. A. Antipov, N. A. Kotov, G. B. Sukhorukov, *J. Mater. Chem.* **2007**, *17*, 1050 – 1054.

[76] a) C. S. Peyratout, L. Dähne, *Angew. Chem. Int. Ed.* **2004**, *43*, 3762 – 3783; *Angew. Chem.* **2004**, *116*, 3850 – 3872; b) P. R. Gil,

L. L. del Mercato, P. del Pino, A. Munoz Javier, W. J. Parak, *Nano Today* **2008**, *3*, 12 – 21.

[77] a) F. Caruso, A. S. Susha, M. Giersig, H. Möhwald, *Adv. Mater.* **1999**, *11*, 950 – 953; b) X. P. Qiu, S. Leporatti, E. Donath, H. Möhwald, *Langmuir* **2001**, *17*, 5375 – 5380; c) G. Berth, A. Voigt, H. Dautzenberg, E. Donath, H. Möhwald, *Biomacromolecules* **2002**, *3*, 579 – 590; d) E. Kharlampieva, S. A. Sukhishvili, *Polym. Rev.* **2006**, *46*, 377 – 395; e) Z. P. Wang, Z. Q. Feng, C. Y. Gao, *Chem. Mater.* **2008**, *20*, 4194 – 4199; f) Y. Zhu, W. J. Tong, C. Y. Gao, *Soft Matter* **2011**, *7*, 5805 – 5815; g) G. K. Such, A. P. R. Johnston, F. Caruso, *Chem. Soc. Rev.* **2011**, *40*, 19 – 29.

[78] a) Y. J. Zhang, S. G. Yang, Y. Guan, W. X. Cao, J. Xu, *Macromolecules* **2003**, *36*, 4238 – 4240; b) Y. Zhu, W. J. Tong, C. Y. Gao, H. Möhwald, *J. Mater. Chem.* **2008**, *18*, 1153 – 1158.

[79] a) A. A. Antipov, G. B. Sukhorukov, *Adv. Colloid Interface Sci.* **2004**, *111*, 49 – 61; b) A. Fery, R. Weinkamer, *Polymer* **2007**, *48*, 7221 – 7235; c) A. P. R. Johnston, G. K. Such, F. Caruso, *Angew. Chem. Int. Ed.* **2010**, *49*, 2664 – 2666; *Angew. Chem.* **2010**, *122*, 2723 – 2725.

[80] a) D. B. Shenoy, A. A. Antipov, G. B. Sukhorukov, H. Möhwald, *Biomacromolecules* **2003**, *4*, 265 – 272; b) N. G. Balabushevich, O. P. Tiourina, D. V. Volodkin, N. I. Larionova, G. B. Sukhorukov, *Biomacromolecules* **2003**, *4*, 1191 – 1197; c) A. S. Angelatos, B. Radt, F. Caruso, *J. Phys. Chem. B* **2005**, *109*, 3071 – 3076; d) Y. Itoh, M. Matsusaki, T. Kida, M. Akashi, *Biomacromolecules* **2006**, *7*, 2715 – 2718.

[81] a) G. Saito, J. A. Swanson, K.-D. Lee, *Adv. Drug Delivery Rev.* **2003**, *55*, 199 – 215; b) A. N. Zelikin, Q. Li, F. Caruso, *Chem. Mater.* **2008**, *20*, 2655 – 2661.

[82] a) S. A. Sukhishvili, *Curr. Opin. Colloid Interface Sci.* **2005**, *10*, 37 – 44; b) S. Anandhakumar, V. Nagaraja, M. R. Ashok, *Colloids Surf. B* **2010**, *78*, 266 – 274; c) B. M. Wohl, J. F. J. Engbersen, *J. Controlled Release* **2012**, *158*, 2 – 14.

[83] a) A. Yu, Y. Wang, E. Barlow, F. Caruso, *Adv. Mater.* **2005**, *17*, 1737 – 1741; b) B. G. De Geest, R. E. Vandenbroucke, A. M. Guenther, G. B. Sukhorukov, W. E. Hennink, N. N. Sanders, J. Demeester, S. C. De Smedt, *Adv. Mater.* **2006**, *18*, 1005 – 1009.

[84] a) A. N. Zelikin, Q. Li, F. Caruso, *Angew. Chem. Int. Ed.* **2006**, *45*, 7743 – 7745; *Angew. Chem.* **2006**, *118*, 7907 – 7909; b) A. N. Zelikin, J. F. Quinn, F. Caruso, *Biomacromolecules* **2006**, *7*, 27 – 30.

[85] a) S. S. Shiratori, M. F. Rubner, *Macromolecules* **2000**, *33*, 4213 – 4219; b) I. Takayuki, K. Toshiyuki, M. Michiya, A. Mitsuru, *Macromolecules* **2010**, *10*, 271 – 277.

[86] a) A. G. Skirtach, C. Dejugnat, D. Braun, A. S. Susha, A. L. Rogach, W. J. Parak, H. Möhwald, G. B. Sukhorukov, *Nano Lett.* **2005**, *5*, 1371 – 1377; b) A. G. Skirtach, A. Muñoz Javier, O. Kreft, K. Köhler, A. Piera Alberola, H. Möhwald, W. J. Parak, G. B. Sukhorukov, *Angew. Chem. Int. Ed.* **2006**, *45*, 4612 – 4617; *Angew. Chem.* **2006**, *118*, 4728 – 4733; c) A. G. Skirtach, P. Karageorgiev, B. G. De Geest, N. Pazos-Perez, D. Braun, G. B. Sukhorukov, *Adv. Mater.* **2008**, *20*, 506 – 510; d) M. F. Bédard, B. G. De Geest, A. G. Skirtach, H. Möhwald, G. B. Sukhorukov, *Adv. Colloid Interface Sci.* **2010**, *158*, 2 – 14; e) A. K. Barman, S. Verma, *Chem. Commun.* **2010**, *46*, 6992 – 6994.

[87] W. Qi, L. Duan, J. B. Li, *Soft Matter* **2011**, *7*, 1571 – 1576.

[88] a) X. L. Yang, X. Han, Y. H. Zhu, *Colloids Surf. A* **2005**, *264*, 49 – 54; b) Q. Zhao, B. Han, Z. Wang, C. Gao, C. Peng, J. Shen, *Nanomedicine* **2007**, *3*, 63 – 74.

[89] a) J. F. Quinn, A. P. R. Johnston, G. K. Such, A. N. Zelikin, F. Caruso, *Chem. Soc. Rev.* **2007**, *36*, 707 – 718; b) J. Shi, Y. Jiang, X. Wang, H. Wu, D. Yang, F. Pan, Y. Suad, Z. Jiang, *Chem. Soc. Rev.* **2014**, *43*, 5192 – 5210.

[90] A. Fujii, Y. Ohmukai, T. Maruyama, T. Sotani, H. Matsuyama, *Colloids Surf. A* **2011**, *384*, 529 – 535.

[91] a) A. P. Johnston, F. Caruso, *Angew. Chem. Int. Ed.* **2007**, *46*, 2677 – 2680; *Angew. Chem.* **2007**, *119*, 2731 – 2734; b) F. Cavalieri, A. Postma, L. Lee, F. Caruso, *ACS Nano* **2009**, *3*, 234 – 240.

[92] A. P. Johnston, L. Lee, Y. Wang, F. Caruso, *Small* **2009**, *5*, 1418 – 1421.

[93] Y. Z. Tian, Y. L. Li, Z. F. Wang, Y. Jiang, *J. Mater. Chem. B* **2014**, *2*, 1667 – 1672.

[94] A. L. Becker, A. P. Johnston, F. Caruso, *Macromol. Biosci.* **2010**, *10*, 488 – 495.

[95] X. Zhang, D. Chabot, Y. Sultan, C. Monreal, M. C. DeRosa, *ACS Appl. Mater. Interfaces* **2013**, *5*, 5500 – 5507.

[96] F. Tanaka, T. Mochizuki, X. Liang, H. Asanuma, S. Tanaka, K. Suzuki, S. Kitamura, A. Nishikawa, K. Ui-Tei, M. Hagiya, *Nano Lett.* **2010**, *10*, 3560 – 3565.

[97] T. Takenaka, M. Endo, Y. Suzuki, Y. Yang, T. Emura, K. Hidaka, T. Kato, T. Miyata, K. Namba, H. Sugiyama, *Chem. Eur. J.* **2014**, *20*, 14951 – 14954.

[98] a) J. H. Jeong, S. W. Kim, T. G. Park, *Bioconjugate Chem.* **2003**, *14*, 473 – 479; b) J. Sánchez-Quesada, A. Saghatelian, S. Cheley, H. Bayley, M. R. Ghadiri, *Angew. Chem. Int. Ed.* **2004**, *43*, 3063 – 3067; *Angew. Chem.* **2004**, *116*, 3125 – 3129.

[99] R. B. Fong, Z. L. Ding, C. J. Long, A. S. Hoffman, P. S. Stayton, *Bioconjugate Chem.* **1999**, *10*, 720 – 725.

[100] J. H. Jeong, T. G. Park, *Bioconjugate Chem.* **2001**, *12*, 917 – 923.

[101] K. Ding, F. E. Alemdaroglu, M. Börsch, R. Berger, A. Herrmann, *Angew. Chem. Int. Ed.* **2007**, *46*, 1172 – 1175; *Angew. Chem.* **2007**, *119*, 1191 – 1194.

[102] F. E. Alemdaroglu, N. C. Alemdaroglu, P. Langguth, A. Herrmann, *Macromol. Rapid Commun.* **2008**, *29*, 326 – 329.

[103] F. E. Alemdaroglu, J. Wang, M. Börsch, R. Berger, A. Herrmann, *Angew. Chem. Int. Ed.* **2008**, *47*, 974 – 976; *Angew. Chem.* **2008**, *120*, 988 – 991.

[104] X. Li, Y. Yu, Q. Ji, L. Qiu, *Nanomed. Nanotech. Biol. Med.* **2015**, *11*, 175 – 184.

[105] C. Wu, T. Chen, D. Han, M. You, L. Peng, S. Cansiz, G. Zhu, C. Li, X. Xiong, E. Jimenez, C. J. Yang, W. Tan, *ACS Nano* **2013**, *7*, 5724 – 5731.

[106] Y. Wu, K. Sefah, H. Liu, R. Wang, W. Tan, *Proc. Natl. Acad. Sci. USA* **2010**, *107*, 5 – 10.

[107] T. Chen, C. S. Wu, E. Jimenez, Z. Zhu, J. G. Dajac, M. You, D. Han, X. Zhang, W. Tan, *Angew. Chem. Int. Ed.* **2013**, *52*, 2012 – 2016; *Angew. Chem.* **2013**, *125*, 2066 – 2070.

[108] F. E. Alemdaroglu, N. C. Alemdaroglu, P. Langguth, A. Herrmann, *Adv. Mater.* **2008**, *20*, 899 – 902.

[109] A. Rodríguez-Pulido, A. I. Kondrachuk, D. K. Prusty, J. Gao, M. A. Loi, A. Herrmann, *Angew. Chem. Int. Ed.* **2013**, *52*, 1008 – 1012; *Angew. Chem.* **2013**, *125*, 1042 – 1046.

[110] Z. Cao, R. Tong, A. Mishra, W. Xu, G. C. Wong, J. Cheng, Y. Lu, *Angew. Chem. Int. Ed.* **2009**, *48*, 6494 – 6498; *Angew. Chem.* **2009**, *121*, 6616 – 6620.

[111] a) D. A. Giljohann, D. S. Seferos, W. L. Daniel, M. D. Massich, P. C. Patel, C. A. Mirkin, *Angew. Chem. Int. Ed.* **2010**, *49*, 3280 – 3294; *Angew. Chem.* **2010**, *122*, 3352 – 3366; b) D. Smith, V. Schüller, C. Engst, J. Rädler, T. Liedl, *Nanomedicine* **2013**, *8*, 105 – 121; c) J. W. de Vries, F. Zhang, A. Herrmann, *J. Controlled Release* **2013**, *172*, 467 – 483.

[112] a) J. Sharma, R. Chhabra, C. S. Andersen, K. V. Gothelf, H. Yan, Y. Liu, *J. Am. Chem. Soc.* **2008**, *130*, 7820 – 7821; b) N. V. Voigt, T. Torring, A. Rotaru, M. F. Jacobsen, J. B. Ravensbaek, R. Subramani, W. Mamdouh, J. Kjems, A. Mokhir, F. Besenbacher, K. V. Gothelf, *Nat. Nanotechnol.* **2010**, *5*, 200 – 203; c) B. Saccà, R. Meyer, M. Erkelenz, K. Kiko, A. Arndt, H. Schroeder, K. S. Rabe, C. M. Niemeyer, *Angew. Chem. Int. Ed.* **2010**, *49*, 9378 – 9383; *Angew. Chem.* **2010**, *122*, 9568 – 9573.

[113] E. S. Andersen, M. Dong, M. M. Nielsen, K. Jahn, R. Subramani, W. Mamdouh, M. M. Golas, B. Sander, H. Stark,

C. L. P. Oliveira, J. S. Pedersen, V. Birkedal, F. Besenbacher, K. V. Gothelf, J. Kjems, *Nature* **2009**, *459*, 73 – 76.
[114] K. Lund, A. J. Manzo, N. Dabby, N. Michelotti, A. Johnso *n*Buck, J. Nangreave, S. Taylor, R. Pei, M. N. Stojanovic, N. G. Walter, E. Winfree, H. Yan, *Nature* **2010**, 465, 206 – 210.
[115] a) S. M. Douglas, I. Bachelet, G. M. Church, *Science* **2012**, *335*, 831 – 834; b) J. Elbaz, I. Willner, *Nat. Mater.* **2012**, *11*, 276 – 277.
[116] O. I. Wilner, Y. Weizmann, R. Gill, O. Lioubashevski, R. Freeman, I. Willner, *Nat. Nanotechnol.* **2009**, *4*, 249 – 254.
[117] R. Orbach, B. Willner, I. Willner, *Chem. Commun.* **2015**, *51*, 4144 – 4160.
[118] a) S. H. Um, J. B. Lee, N. Park, S. Y. Kwon, C. C. Umbach, D. Luo, *Nat. Mater.* **2006**, *5*, 797 – 801; b) E. Cheng, Y. Xing, P. Chen, Y. Yang, Y. Sun, D. Zhou, L. Xu, Q. Fan, D. Liu, *Angew. Chem. Int. Ed.* **2009**, *48*, 7660 – 7663; *Angew. Chem.* **2009**, *121*, 7796 – 7799; c) L. Peng, M. You, Q. Yuan, C. Wu, D. Han, Y. Chen, Z. Zhong, J. Xue, W. Tan, *J. Am. Chem. Soc.* **2012**, *134*, 12302 – 12307; d) C. Wu, D. Han, T. Chen, L. Peng, G. Zhu, M. You, L. Qiu, K. Sefah, X. Zhang, W. Tan, *J. Am. Chem. Soc.* **2013**, *135*, 18644 – 18650; e) W. Guo, C. H. Lu, X. J. Qi, R. Orbach, M. Fadeev, H. H. Yang, I. Willner, *Angew. Chem. Int. Ed.* **2014**, *53*, 10134 – 10138; *Angew. Chem.* **2014**, *126*, 10298 – 10302; f) W. Guo, C. H. Lu, R. Orbach, F. Wang, X. J. Qi, A. Cecconello, D. Seliktar, I. Willner, *Adv. Mater.* **2015**, *27*, 73 – 78.

Received: April 2, 2015
Published online: August 18, 2015

